Long-time behavior of a locally regulated network using random measures on $\mathbb{R}^d$-finite graphs

Khader Khadraoui and Ahmed Sid-Ali
Laval University, Department of Mathematics and Statistics
Québec, Qc, G1V 0A6, Canada

Abstract

A social network can be represented as a geometric graph governed by a spatiotemporal dynamic model using appropriate parameterizations. In this paper we approach the problem of social networks from an interacting particle system perspective. We use a model that describes in continuous time each node of the graph at latent spatial state as a Dirac measure. We describe the model and its formal design as a Markov process on finite and connected geometric graphs with values in path space. A careful analysis of some properties of the underlying model is provided. In particular, we first establish a result on the long-time behavior of the stochastic particle system. Then, the distribution of the network size is investigated and we show that the theory of splines enables us to take into account the evolution of the extinction phenomenon. Our results are validated by a small numerical investigation.

Keywords: Interacting particle systems; Long-time behavior; Monte Carlo; Social networks; Splines.
MSC 2010 subject classifications: Primary 60D05, 60J75, 62G07; secondary 60K35

1 Introduction

A major field of research nowadays is that of adequately studying complex networks thanks to stochastic analysis. In recent years its application area has grown, establishing connections with other fields as diverse as sociology, ecology, biology, genetics, information technology to name a few. For an overview or an account on statistical modeling of random graphs, the reader can find a thorough introduction about static graphs in, e.g., Kolaczyk (2009); Goldenberg et al. (2010) and about dynamic models on graphs in Durrett (2007).

In this paper, we consider a dynamic model using random Poisson measures for social networks on geometric graphs and establish general results on the long-term persistence of activity of the network dynamics. This model - which, inside the interacting particle systems literature, is called

a measure-valued process or at least a particular instance of it - is defined from a geometric graph G (see Penrose (2003) for details) and some recruitment/withdrawal parameters (invitation rate $\alpha > 0$, withdrawal rate $\beta > 0$, and affinity kernel $\mathsf{aff}(x, y)$ between vertices x and y). Let us now introduce notation and recall important facts. Let $G = (\mathcal{V}, \mathcal{E})$ be a graph with undirected edges. Our stochastic generative model on G is a continuous-time Markov process $(\mathscr{N}_\tau)_{\tau \geq 0}$ on the space of subsets of $\mathcal{V}$ where each vertex is characterized by a state x belonging to a closure space $\bar{\mathscr{D}}_G$ of an open connected subset $\mathscr{D}_G$ of $\mathbb{R}^d$, for some $d \geq 1$. By $\mathcal{B}(\bar{\mathscr{D}}_G)$ we denote the σ-algebra of Borel subsets in $\bar{\mathscr{D}}_G$. Let $(\bar{\mathscr{D}}_G, \mathcal{B}(\bar{\mathscr{D}}_G))$ be a locally compact and separable metric space, endowed with a Borel σ-field, state space. Denote by $\mathcal{M}_F(\bar{\mathscr{D}}_G)$ the set of finite measures on $\bar{\mathscr{D}}_G$. In particular, the continuous time and measure-valued social network is given by a point process:

$$\mathscr{N}_\tau = \sum_{i=1}^{N_\tau} \delta_{x_\tau^i}, \qquad \forall\ N_\tau \in \mathbb{N},\ \ \forall\ \tau \in [0, \infty),$$

where $\mathscr{N}_0 \in \mathcal{M}_F(\bar{\mathscr{D}}_G)$ and N_τ stands for the size of the system at time τ. Vertices of the graph (here sometimes referred to as particles) represent individuals. Thus, we investigate a Markov process that evolves according to random Poisson measures (to be introduced later). With this terminology, the dynamics can be described as follows

(*i*) Every vertex not yet withdrawn is assumed to be capable to invite new vertices with positive constant rate α.

(*ii*) The withdrawal rate β is also assumed constant and present vertices stay in the system during random exponential times with mean $1/\beta$ during which they interact with their neighbors following a local affinity function $\mathsf{aff}(x, y)$ of the distance between vertices x and y.

(*iii*) At the end of the presence period, the vertex becomes removed and is no longer considered in the system. The whole system $\mathscr{N}$ represented by the set of all vertices can attract new vertices by affinity with a state variable rate $w^{\mathsf{aff}}(\cdot, \mathscr{N})$.

We begin by presenting some of the properties of the process $(\mathscr{N}_\tau)_{\tau \geq 0}$. For $\mathscr{N} \in \mathcal{M}_F(\bar{\mathscr{D}}_G)$ and for a real-valued bounded measurable function f, we define $\langle \mathscr{N}, f \rangle = \int_{\bar{\mathscr{D}}_G} f d\mathscr{N}$. Let recall that the set of cylindrical functions defined for each $\nu \in \mathcal{M}_F(\bar{\mathscr{D}}_G)$ by $\Phi(\nu) = F\langle \nu, f \rangle$, with $F \in C^1(\mathbb{R})$ and $f \in C(\bar{\mathscr{D}}_G)$ generates the set of bounded measurable functions on $\mathcal{M}_F(\bar{\mathscr{D}}_G)$ as known from (Dawson, 1993, Theorem 3.2.6). The measure-valued process $(\mathscr{N}_t)_{t \geq 0}$ on geometric graph G is

the Markov process on $\bar{\mathscr{D}}_G$ and generator given, for any cylindrical function Φ, by

$$\begin{aligned}\mathscr{A}\Phi(\mathscr{N}) = \alpha \int_{\bar{\mathscr{D}}_G} \mathscr{N}(dx) \int_{\mathbb{R}^d} \Big\{\Phi(\mathscr{N} + \delta_{x+z}) - \Phi(\mathscr{N})\Big\} K^{\mathsf{inv}}(x, dz) \\ + \beta \int_{\bar{\mathscr{D}}_G} \Big\{\Phi(\mathscr{N} - \delta_x) - \Phi(\mathscr{N})\Big\} \mathscr{N}(dx) \\ + \int_{\bar{\mathscr{D}}_G} \Big\{ \int_{\bar{\mathscr{D}}_G} \big(\Phi(\mathscr{N} + \delta_y) - \Phi(\mathscr{N})\big) \mathsf{aff}(x, y) K^{\mathsf{aff}}(dy) \Big\} \mathscr{N}(dx).\end{aligned} \tag{1.1}$$

The above infinitesimal generator $\mathscr{A}$ sums the aging phenomena of the network dynamics. It prescribes that vertices disappear with rate β and join the system by invitation with rate α (their states are dictated by a probability dispersion kernel $K^{\mathsf{inv}}(\cdot, \cdot)$). The third term in (1.1) describes the recruitment by affinity component using a probability dispersion kernel $K^{\mathsf{aff}}(\cdot)$. Note also that the three transition terms of the generator are linear in $\mathscr{N}$. For proofs of these properties and a detailed weak convergence of the model, we refer the reader to Sid-Ali & Khadraoui (2020). Note that representing networks by point processes has created recent advances in statistical analysis of networks, such as graphexes and stretched graphons (Perry & Wolfe, 2013; Veitch & Roy, 2015; Borgs et al., 2018; Caron & Fox, 2017; Yuan et al., 2019).

Our purpose is to study the long-time behavior of the network generative model. The analysis here is somewhat inspired by the long-time study of stochastic network models in the literature (see, i.e., Atar et al. (2021); Mountford et al. (2016); Schapira & Valesin (2017)). By considering recruitment and leaving events occur spontaneously, on finite graphs the activity of the network dynamics eventually may stop. At this point in time known as the extinction time every individual leaves permanently the network. It is noteworthy to say that, for some choices of G, if β is sufficiently large than α and the system is started from a finite number of vertices of the graph, then the extinction time is almost surely (a.s.) finite. In this paper, we give a proof of this phenomenon under much higher generality: we only require β to be above α and the graphs under consideration to be finite graphs of degree bounded by a given number (not to have vertices of arbitrarily large degree; see condition (3.3) in Lemma 1). In other words, if $\alpha \leq \beta$, then the process $\mathscr{N}$ dies out, meaning that for any finite initial configuration, the empty configuration $\sum_{i=1}^{0} \delta_{x^i}$ (i.e., the null measure) is almost surely eventually reached. On the other hand, if $\alpha > \beta$, then the process $\mathscr{N}$ may survive: for any nonempty initial configuration, the event $\{N_\tau \neq 0, \text{ for all } \tau\}$ has positive probability and, conditioned on this event, almost surely any event from the three above events (i), (ii) and (iii) of the dynamics occurs infinitely many times. Note that if we define the extinction time as the stopping time:

$$\tau_0^\star := \inf\{\tau \geq 0, N_\tau = 0\},$$

with the convention $\inf \varnothing = \infty$, then before $\tau_0^\star$ the infinitesimal generator is given by (1.1). After the extinction time $(\mathscr{N}_\tau)_{\tau \geq \tau_0^\star}$ is the null measure, i.e., the system does not contain any particle and the infinitesimal generator is simply reduced to null measure.

The coherence of the use of random measures with network modeling and configuration using random graphs has been recently emphasized as attested by the recent paper of Caron & Fox (2017) about sparse graphs using exchangeable random measures. This paradigm leads to desirable properties and, in particular, to statistical estimation procedures. Importantly, we set here the exact Monte Carlo simulation algorithm of the generative model. By using the nonparametric theory we propose a rigorous decomposition for the distribution of the network size over continuous time. Our estimation methodology based on splines can automatically take into account the presence of extinction and may handle a range of graphs. We show that our method scales to different extinction levels.

The article is organized as follows. In Section 2, after fixing the context within which we work, the design of our particle system approach and its key assumptions are carefully described. The exact Monte Carlo algorithm useful for the numerical computation is given. Moreover, a rigorous pathwise representation of the dynamic in terms of a stochastic differential equation driven by Poisson point measures is given and the infinitesimal generator is derived. In Section 3, we sketch the extinction and survival properties of the system where the long-time behavior of the stochastic particle system is investigated. In Section 4, we deal with the nonparametric inference and we prove that a spline approach approximates efficiently the distribution of the network size for any extinction level and at each time. To validate the computational performance of our results, we present some numerical tests in Section 5.

2 The network model

We start with a microscopic model of state structured network describing the dynamics at the vertex level. We take into account recruitment, either by invitation or by affinity with other individuals not yet present in the network and withdrawal (intrinsic leaving of the network). A long-time behavior of the network is studied. We provide by this way a microscopic justification of the extensive literature on latent space modeling (e.g. Hoff et al. (2002), Penrose (2003) and Hoff (2009)) where by latent space we mean vertices are embedded in a low dimensional, continuous latent space and the probability of an edge is determined by a distance or similarity metric via the latent factors of the vertices. This gives us a better understanding of the large time behavior of the microscopic model and allows us to assess the effects of recruitment and interaction events leading to adaptive dynamics. A lot of statistical models for social networks do not consider time evolution at the vertex level, see Wasserman & Faust (1994), Schweinberger & Snijders (2003), Rastelli et al. (2016), Lusher et al. (2013), Durante et al. (2017) and Hunter et al. (2008). We generalize all these models by introducing a dependence between state and network rates at the vertex level and by taking into account affinity and interaction between vertices, which yields nonlinearity in the limiting phenomena.

2.1 Description of the dynamics

Particles are characterized by their state with values in $\bar{\mathscr{D}}_G$ (a closed subset of $\mathbb{R}^d$). The dispersion of new recruited vertices in the graph G is drawn from some probability dispersion kernels $K^{\mathsf{inv}}(x, dz)$ and $K^{\mathsf{aff}}(dy)$ that induce densities w.r.t. the Lebesgue measure respectively on $\mathbb{R}^d$ and $\bar{\mathscr{D}}_G$ such that these densities are given by $K^{\mathsf{inv}}(x, dz) = k^{\mathsf{inv}}(x, z)dz$ and $K^{\mathsf{aff}}(dy) = k^{\mathsf{aff}}(y)dy$. We describe the whole system by a measure belonging to $\mathcal{M}_F(\bar{\mathscr{D}}_G)$ (the set of finite measures on $\bar{\mathscr{D}}_G$):

$$\mathscr{N}_\tau(dx) = \sum_{i=1}^{N_\tau} \delta_{x_\tau^i}(dx), \tag{2.1}$$

where each vertex in G is represented by a Dirac mass on its state.

Notation 1 *For any measure $\nu(dx)$ defined on $\bar{\mathscr{D}}_G$ and any function $f : \bar{\mathscr{D}}_G \mapsto \mathbb{R}$, we use the angle brackets $\langle \nu, f \rangle$ to denote the function-measure duality, i.e., $\langle \nu, f \rangle = \int_{\bar{\mathscr{D}}_G} f(x)\nu(dx)$. The last notation is valid for continuous measures as well as for point measure $\mathscr{N}_\tau(dx)$ given by (2.1), in the latter case $\langle \mathscr{N}_\tau, f \rangle = \sum_{i=1}^{N_\tau} f(x_\tau^i)$.*

From Notation 1 it's easily seen that $N_\tau = \langle \mathscr{N}_\tau, 1 \rangle = \int_{\bar{\mathscr{D}}_G} \mathscr{N}_\tau(dx)$ is the system size at time $\tau \in \mathbb{R}_+$.

We now describe the three discrete components of the dynamics. A vertex with state $x \in \bar{\mathscr{D}}_G$ in the network described by $\mathscr{N}$ gives invitation to a new vertex with rate $\alpha > 0$. If the invitation is accepted this new vertex immediately becomes a member of the network at state $x + z$ where z is drawn from a probability distribution $k^{\mathsf{inv}}(x, z)dz$ with support on $\bar{\mathscr{D}}_G - \{x\} = \{y - x | y \in \bar{\mathscr{D}}_G\}$ (so that $x + z \in \bar{\mathscr{D}}_G$) and then the system earns one new member ($\mathscr{N} \mapsto \mathscr{N} + \delta_{x+z}$). Each vertex with state $x \in \bar{\mathscr{D}}_G$ can leave the system with rate $\beta > 0$ and the system loses one member ($\mathscr{N} \mapsto \mathscr{N} - \delta_x$). An individual outside the system joins the network by affinity at state y with rate

$$w^{\mathsf{aff}}(y, \mathscr{N}) = \sum_{x \in \mathcal{V} : x \sim y} \mathsf{aff}(x, y) = \int_{\bar{\mathscr{D}}_G} \mathsf{aff}(x, y)\mathscr{N}(dx), \tag{2.2}$$

where $x \sim y$ means that x and y are neighbors and the new state y is drawn from a probability distribution $k^{\mathsf{aff}}(y)dy$ with support on $\bar{\mathscr{D}}_G$. Here, $\mathsf{aff} : \bar{\mathscr{D}}_G \times \bar{\mathscr{D}}_G \to [0, \infty)$ be a real-valued kernel describing the interaction by affinity and assessing the strength of affinity between two vertices. Notice that the recruitment by affinity varies from a state to another since its rate depends on state. Of course, after this recruitment the system earns one new member ($\mathscr{N} \mapsto \mathscr{N} + \delta_y$).

As known, an important concept in the theory of complex networks is the connection between vertices (i.e. the link function) which appears as a main issue in graph theory (Penrose, 2003). To induce vertex heterogeneity in the link function, we endow each vertex with an affinity zone

around it. This zone will be specified by a constant radius $a_{\mathsf{f}} > 0$. Then, for the local affinity function, we consider a linear triangular link model given by

$$\forall x, y \in \bar{\mathscr{D}}_G, \qquad \mathsf{aff}(x,y) = \begin{cases} A_{\mathsf{f}} \left(1 - \frac{1}{a_{\mathsf{f}}} \|x-y\|\right)^+ & \text{if } x \neq y\,, \\ 0 & \text{while if } x = y, \end{cases} \tag{2.3}$$

where $(\cdot)^+ = \max(\cdot, 0)$ and the parameter $A_{\mathsf{f}} > 0$ determines the high affinity level. This straightforward affinity interaction function guarantees to manage that vertex highly connected (with high degree) is of course highly attractive. It's clear that in the graph G we connect two vertices by undirected link if and only if their distance is smaller than a certain neighborhood threshold of affinity a_{f} that is independent of state. Furthermore, one could imagine more complex affinity models when more complex scenarios are investigated but here we restrict ourselves to this choice due to some technical reasons in the long-time behavior investigation (we will show a result that holds over connection functions that are zero beyond the affinity threshold).

Let us mention different forms for the recruitment, withdrawal and interaction rates that can be found in the literature to build network models (Aldous, 1997; Norros & Reittu, 2006; Bollobás et al., 2007; van der Hofstad, 2017). A generalization by considering rates $\alpha(x)$ and $\beta(x)$ with $x \in \bar{\mathscr{D}}_G$ might allow us to take into account external effects such as attractive vertices (hubs), unattractive vertices and so forth. For the interaction kernel $\mathsf{aff}(\cdot,\cdot)$, a particular case is the (density dependent) logistic one, for which the interaction exerted on a vertex state is then proportional to the total number of vertices in the network, and thus nonlocal. Moreover, we can cite also the class of connection functions that decay exponentially in some fixed positive power of distance. In some applications, it is desirable to use the Rayleigh fading connection function given by $\exp(-a(\|x-y\|/b)^c)$ for some fixed positive $a, b, c > 0$ (typically $c = 2$). It would be interesting to extend our results to these connection functions.

A natural hypothesis that will be considered from now on is to assume that these mechanisms of recruitment with dispersion and withdrawal are mutually independent. Nevertheless, considering individual exponential clocks is relatively cumbersome and a better efficient Monte Carlo procedure will rely on the existence of one global exponential clock that dominates all point phenomena. That existence holds true when all the different individual clocks are uniformly bounded. For simplicity, we assume from now on that the spatial dependence of the introduced kernels and rates is bounded in the sense of Assumption 1.

Assumption 1 *Assume that there exist some positive reals γ_1, γ_2 and some probability densities $\tilde{k}^{\mathsf{inv}}$ on $\mathbb{R}^d$ and $\tilde{k}^{\mathsf{aff}}$ on $\bar{\mathscr{D}}_G$ such that*

$$k^{\mathsf{inv}}(x,z) \leq \gamma_1 \tilde{k}^{\mathsf{inv}}(z) \qquad \text{and} \qquad k^{\mathsf{aff}}(y) \leq \gamma_2 \tilde{k}^{\mathsf{aff}}(y), \tag{2.4}$$

for all $x, y \in \bar{\mathscr{D}}_G$ and $z \in \mathbb{R}^d$. As well, for all $\mathscr{N} \in \mathcal{M}_F(\bar{\mathscr{D}}_G)$, we assume that there exists a constant $A_{\mathsf{f}} > 0$ such that

$$\mathsf{aff}(x,y) \leq A_{\mathsf{f}} \qquad \text{which implies} \qquad w^{\mathsf{aff}}(y, \mathscr{N}) \leq A_{\mathsf{f}} N. \tag{2.5}$$

Under Assumption 1, the generative point process $\mathscr{N}$ can be obtained as the unique strong solution of a stochastic differential equation (SDE) driven by the following three Poisson point measures (PPMs) corresponding to the dynamics described above.

Let $\mathscr{N}_0$ denotes the initial condition of the process, it is a random variable with values in $\mathcal{M}_F(\bar{\mathscr{D}}_G)$. We write $|A|$ to denote the cardinality of a set A. The model has a vector $\Lambda = (\alpha, \beta, A_{\mathsf{f}}, a_{\mathsf{f}}, \Lambda^{\mathsf{inv}}, \Lambda^{\mathsf{aff}})$ of unknown parameters, assumed to lie in $(\mathbb{R}_+^*)^4 \times \mathbb{R}^{|\Lambda^{\mathsf{inv}}|+|\Lambda^{\mathsf{aff}}|}$ where Λ^{inv} denotes the parameter set of the invitation dispersion kernel and Λ^{aff} denotes the parameter set of the affinity dispersion kernel. We also denote by $\mathbb{P}_\Lambda$ a probability measure under which the process with parameter set Λ is defined on the graph G; later to avoid overly burdensome notation we omit Λ from the notation as well. We denote by $\mathbb{E}_\Lambda$, or simply $\mathbb{E}$, the associated expectation. Let $(\Omega, \mathcal{A}, \mathbb{P})$ be a sufficiently large probability space. On this probability space, let consider the following basic independent PPMs:

(*i*) Let P^α be a PPM on $[0,\infty) \times \mathbb{N}^* \times \mathbb{R}^d \times [0,1]$ of intensity measure:

$$I^\alpha(dt, di, dz, d\rho) = \alpha\gamma_1 \tilde{k}^{\mathsf{inv}}(z) dt \Big(\sum_{k\geq 1} \delta_k(di) \Big) dz d\rho,$$

where $dt, dz, d\rho$ are the Lebesgue measures on, respectively, $[0,\infty), \mathbb{R}^d, [0,1]$, and $\sum_{k\geq 1} \delta_k(di)$ is the counting measure on $\mathbb{N}^*$.

(*ii*) Let P^β be a PPM on $[0,\infty) \times \mathbb{N}^* \times [0,1]$ of intensity measure:

$$I^\beta(dt, di, d\rho) = \beta dt \Big(\sum_{k\geq 1} \delta_k(di) \Big) d\rho.$$

(*iii*) Let P^{aff} be a PPM on $[0,\infty) \times \mathbb{N}^* \times \bar{\mathscr{D}}_G \times [0,1]$ of intensity measure:

$$I^{\mathsf{aff}}(dt, di, dy, d\rho) = A_{\mathsf{f}}\gamma_2 \tilde{k}^{\mathsf{aff}}(y) dt \Big(\sum_{k\geq 1} \delta_k(di) \Big) dy d\rho.$$

Some comments are in order about the above PPMs. The first invitation point measure P^α provides possible times at which invitation recruitment may occur. Each of its atoms is associated with a possible invitation event time t, a real z which gives the dispersion of the vertex being possibly recruited and an integer i which gives the vertex that has to produce the invitation. The mark ρ is an auxiliary variable used for the construction of an acceptance/rejection Monte Carlo sampling (to be specified later). Similar interpretation holds for P^β and P^{aff}. We consider the canonical filtration $(\mathcal{F}_\tau)_{\tau\geq 0}$ generated by P^α, P^β, P^{aff} and $\mathscr{N}_0$. (Notice that we suppose that the above PPMs and $\mathscr{N}_0$ are mutually independent). We denote by $\mathscr{N}_{\tau-}$the network process at time τ before any possible event and by $\mathbb{1}_A$ the indicator function of the set A.

We introduce now explicitly a SDE driven by the above PPMs, for which the existence and the uniqueness of the solution are stated. The solution is a Markov process, with generator (1.1) that corresponds to the dynamics described previously and gives a rigorous pathwise representation of the model in terms of PPMs.

Definition 1 *Assume that conditions* (2.4) *and* (2.5) *hold. The point process* $\mathscr{N}_\tau$ *is a* $(\mathcal{F}_\tau)_\tau$*-adapted stochastic process described by:*

$$\begin{aligned}\mathscr{N}_\tau =& \mathscr{N}_0 + \int_0^\tau \int_{\mathbb{N}^*} \int_{\mathbb{R}^d} \int_0^1 \mathbb{1}_{\{i\le N_{t-}\}} \mathbb{1}_{\left\{\rho\le (k^{\mathsf{inv}}(x^i_{t-},z))\big/(\gamma_1 \tilde{k}^{\mathsf{inv}}(z))\right\}} \delta_{(x^i_{t-}+z)} P^\alpha(dt,di,dz,d\rho) \\ &- \int_0^\tau \int_{\mathbb{N}^*} \int_0^1 \mathbb{1}_{\{i\le N_{t-}\}} \mathbb{1}_{\{\rho\le(\beta/\beta)\}} \delta_{(x^i_{t-})} P^\beta(dt,di,d\rho) \\ &+ \int_0^\tau \int_{\mathbb{N}^*} \int_{\bar{\mathscr{D}}_G} \int_0^1 \mathbb{1}_{\{i\le N_{t-}\}} \mathbb{1}_{\left\{\rho\le(\mathsf{aff}(x^i_{t-},y)k^{\mathsf{aff}}(y))\big/(A_{\mathsf{f}}\gamma_2\tilde{k}^{\mathsf{aff}}(y))\right\}} \delta_{(y)} P^{\mathsf{aff}}(dt,di,dy,d\rho),\end{aligned} \tag{2.6}$$

where the three terms of integrals are associated to the three basic independent mechanisms.

Now, we state in Theorem 1 that if the network process $\mathscr{N}$ solves (2.6), then it follows the dynamic described by the infinitesimal generator $\mathscr{A}$ given by (1.1).

Theorem 1 *Assume that conditions* (2.4) *and* (2.5) *are satisfied. Consider a* $(\mathcal{F}_\tau)_{\tau\ge0}$*-adapted stochastic process* $(\mathscr{N}_\tau)_{\tau\ge0}$ *that solves* (2.6)*. Then* $(\mathscr{N}_\tau)_{\tau\ge0}$ *is Markovian and its infinitesimal generator* $\mathscr{A}$ *is defined, in particular for the class of test functions* Φ*, by expression* (1.1)*.*

Proof The proof for the fact that $(\mathscr{N}_\tau)_{\tau\ge0}$ is Markovian is classical and it will be omitted. For the class of test functions Φ and all $\tau\ge0$, $\Phi(\mathscr{N}_\tau)$ is given a.s. by

$$\begin{aligned}\Phi(\mathscr{N}_\tau) = \Phi(\mathscr{N}_0) &+ \int_0^\tau \int_{\mathbb{N}^*} \int_{\mathbb{R}^d} \int_0^1 \mathbb{1}_{\{i\le N_{t-}\}} \mathbb{1}_{\{\rho\le(k^{\mathsf{inv}}(x^i_{t-},z))/(\gamma_1\tilde{k}^{\mathsf{inv}}(z))\}} \\ &\qquad \times [\Phi(\mathscr{N}_{t-} + \{\delta_{(x^i_{t-}+z)}\}) - \Phi(\mathscr{N}_{t-})] P^\alpha(dt,di,dz,d\rho) \\ &+ \int_0^\tau \int_{\mathbb{N}^*} \int_0^1 \mathbb{1}_{\{i\le N_{t-}\}} \mathbb{1}_{\{\rho\le(\beta/\beta)\}} \\ &\qquad \times [\Phi(\mathscr{N}_{t-} - \{\delta_{(x^i_{t-})}\}) - \Phi(\mathscr{N}_{t-})] P^\beta(dt,di,d\rho) \\ &+ \int_0^\tau \int_{\mathbb{N}^*} \int_{\bar{\mathscr{D}}_G} \int_0^1 \mathbb{1}_{\{i\le N_{t-}\}} \mathbb{1}_{\{\rho\le(\mathsf{aff}(x^i_{t-},y)k^{\mathsf{aff}}(y))/(A_{\mathsf{f}}\gamma_2\tilde{k}^{\mathsf{aff}}(y))\}} \\ &\qquad \times [\Phi(\mathscr{N}_{t-} + \{\delta_{(y)}\}) - \Phi(\mathscr{N}_{t-})] P^{\mathsf{aff}}(dt,di,dy,d\rho).\end{aligned} \tag{2.7}$$

Let us consider the given intensities of the PPMs and take the expectation of (2.7) which enable us to write

$$
\begin{aligned}
\mathbb{E}[\Phi(\mathscr{N}_\tau)] &= \mathbb{E}[\Phi(\mathscr{N}_0)] + \int_0^\tau \mathbb{E}\Big[\alpha\gamma_1\tilde{k}^{\mathsf{inv}}(z)\sum_{i=1}^{N_{t-}}\frac{1}{\gamma_1\tilde{k}^{\mathsf{inv}}(z)} \\
&\qquad \times \int_{\mathbb{R}^d}\Big\{\Phi(\mathscr{N}_{t-}+\{\delta_{(x^i_{t-}+z)}\}) - \Phi(\mathscr{N}_{t-})\Big\}k^{\mathsf{inv}}(x^i_{t-},z)dz\Big]dt \\
&\quad + \int_0^\tau \mathbb{E}\Big[\beta\sum_{i=1}^{N_{t-}}\frac{\beta}{\beta}\Big\{\Phi(\mathscr{N}_{t-}-\{\delta_{(x^i_{t-})}\}) - \Phi(\mathscr{N}_{t-})\Big\}\Big]dt \\
&\quad + \int_0^\tau \mathbb{E}\Big[A_{\mathsf{f}}\gamma_2\tilde{k}^{\mathsf{aff}}(y)\sum_{i=1}^{N_{t-}}\frac{1}{A_{\mathsf{f}}\gamma_2\tilde{k}^{\mathsf{aff}}(y)} \\
&\qquad \times \int_{\bar{\mathscr{D}}_G}\Big\{\Phi(\mathscr{N}_{t-}+\{\delta_{(y)}\}) - \Phi(\mathscr{N}_{t-})\Big\}\mathsf{aff}(x^i_{t-},y)k^{\mathsf{aff}}(y)dy\Big]dt \\
&= \mathbb{E}[\Phi(\mathscr{N}_0)] + \beta\int_0^\tau \mathbb{E}\Big[\int_{\bar{\mathscr{D}}_G}\mathscr{N}_t(dx)\Big\{\Phi(\mathscr{N}_t-\{\delta_{(x)}\}) - \Phi(\mathscr{N}_t)\Big\}\Big]dt \\
&\quad + \alpha\int_0^\tau \mathbb{E}\Big[\int_{\bar{\mathscr{D}}_G}\mathscr{N}_t(dx)\int_{\mathbb{R}^d}\Big\{\Phi(\mathscr{N}_t+\{\delta_{(x+z)}\}) - \Phi(\mathscr{N}_t)\Big\}k^{\mathsf{inv}}(x,z)dz\Big]dt \qquad (2.8) \\
&\quad + \int_0^\tau \mathbb{E}\Big[\int_{\bar{\mathscr{D}}_G}\Big\{\int_{\bar{\mathscr{D}}_G}\big(\Phi(\mathscr{N}_t+\delta_{(y)}) - \Phi(\mathscr{N}_t)\big)\mathsf{aff}(x,y)k^{\mathsf{aff}}(y)dy\Big\}\mathscr{N}_t(dx)\Big]dt.
\end{aligned}
$$

Now, differentiating the expression (2.8) at $\tau = 0$ and using $\mathscr{A}\Phi(\mathscr{N}_0) = \partial_\tau\mathbb{E}[\Phi(\mathscr{N}_\tau)]_{\tau=0}$ lead immediately to (1.1). This completes the proof. □

We carry on first with showing the existence and uniqueness of the stochastic process $(\mathscr{N}_\tau)_{\tau\geq 0}$ in the sense of Definition 1. We begin by a moment estimates result concerning the size evolution of the system. Second, we will deduce that existence and uniqueness of a strong solution of the SDE driven by the PPMs (2.6) follow as a consequence. Note that the size properties for this class of point measures have been largely studied in the literature. More importantly, the following Theorem 2 proves that the size of the vertices will grow with bound which guarantees that the system does not explode.

Theorem 2 *Admit assumptions (2.4) and (2.5). Consider that* $\mathbb{E}[\langle\mathscr{N}_0,1\rangle^m] < \infty$ *for some* $m \geq 1$*, then for any* $0 < T < \infty$*:*

$$
\mathbb{E}\Big[\sup_{\tau\in[0,T]}\langle\mathscr{N}_\tau,1\rangle^m\Big] < \infty. \qquad (2.9)
$$

Proof First, a computation using $\Phi(\mathscr{N}) = \langle \mathscr{N}, 1\rangle^m$ in (2.7) (by setting $f = 1$ and $F(x) = x^m$) shows that

$$\begin{aligned}\langle \mathscr{N}_\tau, 1\rangle^m \le \langle \mathscr{N}_0, 1\rangle^m &+ \int_0^\tau \int_{\mathbb{N}^*} \int_{\mathbb{R}^d} \int_0^1 \mathbb{1}_{\{i\le \langle \mathscr{N}_{t-},1\rangle\}} \mathbb{1}_{\{\rho \le (k^{\mathsf{inv}}(x^i_{t-},z))/(\gamma_1 \tilde{k}^{\mathsf{inv}}(z))\}} \\ &\qquad \Big((\langle \mathscr{N}_{t-},1\rangle + 1)^m - \langle \mathscr{N}_{t-},1\rangle^m \Big) P^\alpha(dt,di,dz,d\rho) \\ &+ \int_0^\tau \int_{\mathbb{N}^*} \int_{\bar{\mathscr{D}}_G} \int_0^1 \mathbb{1}_{\{i\le \langle \mathscr{N}_{t-},1\rangle\}} \mathbb{1}_{\{\rho \le (\mathsf{aff}(x^i_{t-},y) k^{\mathsf{aff}}(y))/A_{\mathsf{f}}\gamma_2 \tilde{k}^{\mathsf{aff}}(y)\}} \\ &\qquad \Big((\langle \mathscr{N}_{t-},1\rangle + 1)^m - \langle \mathscr{N}_{t-},1\rangle^m \Big) \quad P^{\mathsf{aff}}(dt,di,dy,d\rho),\end{aligned} \tag{2.10}$$

where the inequality holds by neglecting the following nonpositive withdrawal term

$$\int_0^\tau \int_{\mathbb{N}^*} \int_0^1 \mathbb{1}_{\{i\le \langle \mathscr{N}_{t-},1\rangle\}} \mathbb{1}_{\{\rho \le (\beta/\beta)\}} \times \Big((\langle \mathscr{N}_{t-},1\rangle - 1)^m - \langle \mathscr{N}_{t-},1\rangle^m \Big) P^\beta(dt,di,d\rho) < 0.$$

For any $n \in \mathbb{N}^*$, we consider the stopping time $\tau_n = \inf\{\tau \ge 0, \langle \mathscr{N}_\tau, 1\rangle \ge n\}$. Moreover, note that the right side of the inequality (2.10) is a nondecreasing process (with two recruitment components) and then, by using the notation $A \wedge B = \min(A, B)$ for any $A, B \in \mathbb{R}$, we find

$$\begin{aligned}\sup_{t\in[0,\tau\wedge\tau_n]} \langle \mathscr{N}_t, 1\rangle^m \le \langle \mathscr{N}_0, 1\rangle^m &+ \int_0^{\tau\wedge\tau_n} \int_{\mathbb{N}^*} \int_{\mathbb{R}^d} \int_0^1 \mathbb{1}_{\{i\le \langle \mathscr{N}_{t-},1\rangle\}} \mathbb{1}_{\{\rho \le (k^{\mathsf{inv}}(x^i_{t-},z))/(\gamma_1 \tilde{k}^{\mathsf{inv}}(z))\}} \\ &\qquad \Big((\langle \mathscr{N}_{t-},1\rangle + 1)^m - \langle \mathscr{N}_{t-},1\rangle^m \Big) P^\alpha(dt,di,dz,d\rho) \\ &+ \int_0^{\tau\wedge\tau_n} \int_{\mathbb{N}^*} \int_{\bar{\mathscr{D}}_G} \int_0^1 \mathbb{1}_{\{i\le \langle \mathscr{N}_{t-},1\rangle\}} \mathbb{1}_{\{\rho \le (\mathsf{aff}(x^i_{t-},y) k^{\mathsf{aff}}(y))/A_{\mathsf{f}}\gamma_2 \tilde{k}^{\mathsf{aff}}(y)\}} \\ &\qquad \Big((\langle \mathscr{N}_{t-},1\rangle + 1)^m - \langle \mathscr{N}_{t-},1\rangle^m \Big) \quad P^{\mathsf{aff}}(dt,di,dy,d\rho) \\ \le \langle \mathscr{N}_0, 1\rangle^m &+ C_m \int_0^{\tau\wedge\tau_n} \int_{\mathbb{N}^*} \int_{\mathbb{R}^d} \int_0^1 \mathbb{1}_{\{i\le \langle \mathscr{N}_{t-},1\rangle\}} \mathbb{1}_{\{\rho \le (k^{\mathsf{inv}}(x^i_{t-},z))/(\gamma_1 \tilde{k}^{\mathsf{inv}}(z))\}} \\ &\qquad (\langle \mathscr{N}_{t-},1\rangle^{m-1} + 1) P^\alpha(dt,di,dz,d\rho) \\ &+ C_m \int_0^{\tau\wedge\tau_n} \int_{\mathbb{N}^*} \int_{\bar{\mathscr{D}}_G} \int_0^1 \mathbb{1}_{\{i\le \langle \mathscr{N}_{t-},1\rangle\}} \mathbb{1}_{\{\rho \le (\mathsf{aff}(x^i_{t-},y) k^{\mathsf{aff}}(y))/A_{\mathsf{f}}\gamma_2 \tilde{k}^{\mathsf{aff}}(y)\}} \\ &\qquad (\langle \mathscr{N}_{t-},1\rangle^{m-1} + 1) \quad P^{\mathsf{aff}}(dt,di,dy,d\rho),\end{aligned}$$

where the last inequality holds by using the inequality $(x+1)^m - x^m \le C_m(x^{m-1} + 1)$ for some constant C_m that will change from line to line in the sequel. Now, by taking expectation and

using the optional stopping theorem, we obtain,

$$\begin{aligned}
\mathbb{E}\Big[\sup_{t\in[0,\tau\wedge\tau_n]}\langle\mathscr{N}_t,1\rangle^m\Big] &\leq \mathbb{E}[\langle\mathscr{N}_0,1\rangle^m] + C_m\int_0^\tau \mathbb{E}\Big[\mathbb{1}_{\{t\leq\tau\wedge\tau_n\}}\int_{\mathbb{R}^d}\alpha\gamma_1\tilde{k}^{\mathsf{inv}}(z)dz(\langle\mathscr{N}_{t-},1\rangle^m+\langle\mathscr{N}_{t-},1\rangle)\Big]dt\\
&\quad + C_m\int_0^\tau \mathbb{E}\Big[\mathbb{1}_{\{t\leq\tau\wedge\tau_n\}}\int_{\bar{\mathscr{D}}_G} A_{\mathsf{f}}\gamma_2\tilde{k}^{\mathsf{aff}}(y)dy(\langle\mathscr{N}_{t-},1\rangle^m+\langle\mathscr{N}_{t-},1\rangle)\Big]dt\\
&\leq \mathbb{E}[\langle\mathscr{N}_0,1\rangle^m] + C_m\int_0^\tau \mathbb{E}\Big[(\langle\mathscr{N}_{t\wedge\tau_n},1\rangle^m+1)\Big]dt\\
&\quad + C_m\int_0^\tau \mathbb{E}\Big[(\langle\mathscr{N}_{t\wedge\tau_n},1\rangle^m+1)\Big]dt\\
&\leq \mathbb{E}[\langle\mathscr{N}_0,1\rangle^m] + 3C_m\int_0^\tau \mathbb{E}\Big[\langle\mathscr{N}_{t\wedge\tau_n},1\rangle^m\Big]dt.
\end{aligned}$$

Applying Gronwall's lemma, for any $T<\infty$, gives

$$\mathbb{E}\Big[\sup_{\tau\in[0,T\wedge\tau_n]}\langle\mathscr{N}_\tau,1\rangle^m\Big] \leq \mathbb{E}[\langle\mathscr{N}_0,1\rangle^m]\exp(3C_mT) = C_{m,T}, \tag{2.11}$$

where clearly the constant $C_{m,T}$ do not depend on n. First, we deduce from (2.11) that $\tau_n\xrightarrow{a.s.}\infty$. Indeed, if not, we can find $T^*<\infty$ such that:

$$P_{T^*} = \mathbb{P}(\sup_n\tau_n < T^*) > 0.$$

This would imply that for each n:

$$\begin{aligned}
\mathbb{E}\Big[\sup_{\tau\in[0,T\wedge\tau_n]}\langle\mathscr{N}_\tau,1\rangle^m\Big] &= \mathbb{E}\Big[\sup_{\tau\in[0,T\wedge\tau_n]}\langle\mathscr{N}_\tau,1\rangle^m\mathbb{1}_{\{\sup_n\tau_n<T^*\}}\Big] + \mathbb{E}\Big[\sup_{\tau\in[0,T\wedge\tau_n]}\langle\mathscr{N}_\tau,1\rangle^m\mathbb{1}_{\{\sup_n\tau_n\geq T^*\}}\Big]\\
&\geq \mathbb{E}\Big[\sup_{\tau\in[0,T\wedge\tau_n]}\langle\mathscr{N}_\tau,1\rangle^m\mathbb{1}_{\{\sup_n\tau_n<T^*\}}\Big]\\
&= n^mP_{T^*},
\end{aligned}$$

which contradicts (2.11). Finally, from Fatou's lemma we conclude that:

$$\begin{aligned}
\mathbb{E}\Big[\sup_{\tau\in[0,T]}\langle\mathscr{N}_\tau,1\rangle^m\Big] &= \mathbb{E}\Big[\liminf_{n\to\infty}\sup_{\tau\in[0,T\wedge\tau_n]}\langle\mathscr{N}_\tau,1\rangle^m\Big]\\
&\leq \liminf_{n\to\infty}\mathbb{E}\Big[\sup_{\tau\in[0,T\wedge\tau_n]}\langle\mathscr{N}_\tau,1\rangle^m\Big]\\
&\leq C_{m,T},
\end{aligned}$$

which completes the proof. □

An immediate consequence of Theorem 2 is the existence and uniqueness of the process $(\mathscr{N}_\tau)_{\tau\geq0}$ in the sense of SDE (2.6).

Corollary 1 *Assume that* (2.4) *and* (2.5) *hold and that* $\mathbb{E}[\langle\mathscr{N}_0,1\rangle]<\infty$. *Then there exists a unique process* $(\mathscr{N}_\tau)_{\tau\geq0}$ *in the sense of Definition* 1.

Proof Existence holds as we can construct $(\mathscr{N}_\tau)_{\tau\geq 0}$ using a Monte Carlo algorithm (see Section (2.2) for a pseudocode of this algorithm), where the events are chosen thanks to an acceptance/rejection principle according to the PPMs P^α, P^β and P^{aff}. It remains only to verify that the jump instant sequence T_k tends a.s. to infinity, and this follows from (2.9) with $m = 1$. Indeed, if not, we can find $\bar{T}$ such that $\lim_{k\to\infty} T_k < \bar{T}$. This would imply, given the accumulation of an infinite number of events in the interval $[0, \bar{T}]$, that, for all n,

$$\mathbb{P}(\sup_{\tau\in[0,\bar{T}]} \langle \mathscr{N}_\tau, 1\rangle > n) > 0.$$

Therefore, by Markov inequality,

$$\mathbb{E}[\sup_{\tau\in[0,\bar{T}]} \langle \mathscr{N}_\tau, 1\rangle] > n\mathbb{P}(\sup_{\tau\in[0,\bar{T}]} \langle \mathscr{N}_\tau, 1\rangle > n),$$

which contradicts (2.9) with $m = 1$ and then proves that $T_k \to \infty$. Finally, uniqueness also holds, since we have no choice in the construction. □

2.2 Algorithm and graphical configuration

The distribution (law) of the network process is characterized by its infinitesimal generator (1.1). This characterization is relatively abstract, so we subsequently propose now to design an exact Monte Carlo algorithm that simulates the network and provides an empirical representation of its law. The method is exact as, up to the pseudo-random numbers generator approximation, it generates a network that has the same distribution as the considered Markov process $(\mathscr{N}_\tau)_{\tau\geq 0}$.

Let $T > 0$ and let us consider the evolution system on the compact time interval $[0, T]$. Given a vertex chosen at random in the system, the type of point phenomenon to be considered is determined by a sampling technique, and it is decided whether the chosen phenomenon is actually applied or not by an acceptance/rejection sampling technique. Vertices in the graph G generated by the process $\mathscr{N}$ are independent of each other. Each vertex in the state x has three independent exponential clocks that control the occurrence of the events. Straightforwardly, an efficient Monte Carlo procedure consists of the existence of one global clock, that models all point mechanisms, computed easily thanks to the properties of the exponential distribution by,

$$\mathsf{H}_\tau = \mathsf{h}_\tau^\alpha + \mathsf{h}_\tau^{\mathsf{aff}} + \mathsf{h}_\tau^\beta, \qquad \text{where} \quad \begin{cases} \mathsf{h}_\tau^\alpha = \alpha N_\tau, \\ \mathsf{h}_\tau^{\mathsf{aff}} = A_{\mathsf{f}} N_\tau, \\ \mathsf{h}_\tau^\beta = \beta N_\tau. \end{cases} \tag{2.12}$$

Let $T_0 = 0$ and start with a randomly chosen initial state $\mathscr{N}_0$. For $k = 1, 2, 3, \ldots$, suppose the time of the last event T_{k-1} and the corresponding state of the system $\mathscr{N}_{T_{k-1}}$ given, we describe how to simulate $\mathscr{N}_{T_k}$ starting from $\mathscr{N}_{T_{k-1}}$, for $k = 1, 2, 3, \ldots, n$ with $T_n = T$ a stopping time. In order to determine the instant T_k when the next event could take place, we draw one realization from the exponential distribution with parameter $\mathsf{H}_{T_{k-1}}$ using (2.12). Then, from the instant T_{k-1}

Algorithm 1 Exact Monte Carlo simulation of the modeling by random measures

Draw initial condition of the process $\mathscr{N}_0$ and set $T_0 \leftarrow 0$
for $k = 1, 2, ..., n$ **do**
  $\mathsf{H}_{T_{k-1}} \leftarrow (\mathsf{h}^{\alpha}_{T_{k-1}} + \mathsf{h}^{\mathsf{aff}}_{T_{k-1}} + \mathsf{h}^{\beta}_{T_{k-1}})$
  $\Delta t_k \sim \exp(H_{T_{k-1}})$
  $T_k \leftarrow T_{k-1} + \Delta t_k$
  Compute the three probabilities: $\rho^{\alpha}_k \leftarrow \frac{\mathsf{h}^{\alpha}_{T_{k-1}}}{\mathsf{H}_{T_{k-1}}}$; $\rho^{\mathsf{aff}}_k \leftarrow \frac{\mathsf{h}^{\mathsf{aff}}_{T_{k-1}}}{\mathsf{H}_{T_{k-1}}}$; $\rho^{\beta}_k \leftarrow \frac{\mathsf{h}^{\beta}_{T_{k-1}}}{\mathsf{H}_{T_{k-1}}}$
  $u \sim U[0, 1]$
  if $u \in [0, \rho^{\alpha}_k]$ **then**
    $i \sim U\{1, ..., N_{T_{k-1}}\}$
    $z \sim K^{\mathsf{inv}}(x^i_{T_{k-1}}, dz)$
    $\mathscr{N}_{T_k} \leftarrow \mathscr{N}_{T_{k-1}} + \delta_{x^i_{T_{k-1}}+z}$ % recruitment by invitation
  else
    if $u \in (\rho^{\alpha}_k, \rho^{\alpha}_k + \rho^{\beta}_k]$ **then**
      $i \sim U\{1, ..., N_{T_{k-1}}\}$
      $\mathscr{N}_{T_k} \leftarrow \mathscr{N}_{T_{k-1}} - \delta_{x^i_{T_{k-1}}}$ % withdrawn of vertex at state $x^i_{T_{k-1}}$
    else
      $y \sim K^{\mathsf{aff}}(dy)$
      $i \sim U\{1, ..., N_{T_{k-1}}\}$
      $u' \sim U[0, 1]$
      if $u' \leq \frac{\mathsf{aff}(x^i_{T_{k-1}}, y)k^{\mathsf{aff}}(y)}{A_{\mathsf{f}}\gamma_2 \tilde{k}^{\mathsf{aff}}(y)}$ **then**
        $\mathscr{N}_{T_k} \leftarrow \mathscr{N}_{T_{k-1}} + \delta_y$ % recruitment by affinity
      end if
    end if
  end if
end for

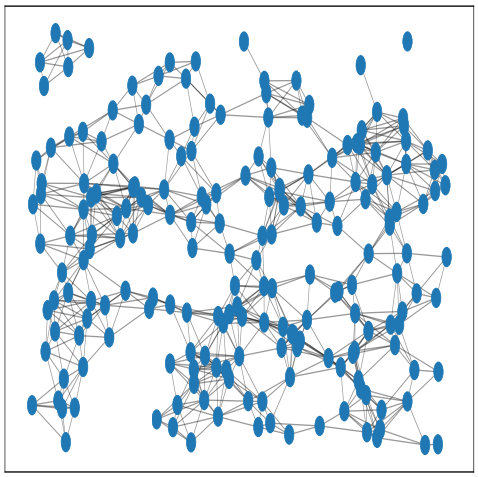

Figure 1: Geometric graph shown a state of the network process in the unit square (here $\bar{\mathscr{D}}_G = [0,1]^2$, $N = 198$ and $a_{\mathsf{f}} = 0.125$). Vertices are indicated by small circles and connected by linear lines (edges) if the intervertex distance is small than 0.125.

to the instant T_k of the next event, i.e., along the time interval $[T_{k-1}, T_k)$ nothing is happening and the iterations of the scheme describing the occurrence of events are given in Algorithm 1.

We introduce now the configuration with geometric graphs. Accordingly, we are interested, as an illustrative example, in constructing a random geometric graph on one state of the network with size $N = 198$ particles in the unit square ($\bar{\mathscr{D}}_G = [0,1]^2$) and with affinity threshold $a_{\mathsf{f}} = 0.125$. As shown, the particles $x^1, \ldots, x^{198}$ are related through a random network and are represented by the vertices of an undirected graph. Between two neighbors, we place an edge if $\|x^i - x^j\| \leq a_{\mathsf{f}}$, for any $i \neq j$, to highlight the affinity interaction mechanism (see Figure 1).

In the next section, we shall study the long-time behavior of the process based on the random measures described previously and we state our main result.

3 Long-time behavior

After fixing the model within which we work (its existence, uniqueness and algorithmic construction), we investigate now the crucial question related to the long-time behavior of the empirical measure (2.1). At first glance, we refer the interested reader to Liggett (1985) for an amount of techniques and classical results about the survival and extinction properties concerning the interacting particle systems. Notice that the contact process (which is one of the most studied interacting particle systems) was introduced recently in the graph theory and a plethora

of contact process models have been proposed in the literature about random networks like configuration models, or preferential attachment graphs (Durrett, 2007; Chatterjee & Durrett, 2009; Mountford et al., 2013; Schapira & Valesin, 2017).

First, we gather a brief treatment of some properties useful for better understanding the generative process and keep forthcoming analysis more clear. We state in the sequel a result that shows essentially that if there is at most one vertex at each state at time $\tau = 0$ which means that a.s.

$$\sup_{x\in\bar{\mathscr{D}}_G} \mathscr{N}_0(\{x\}) \leq 1, \tag{3.1}$$

then this also holds for all $\tau \geq 0$.

Proposition 1 *Assume that conditions (2.4), (2.5) and (3.1) hold. Suppose that* $\mathbb{E}[\langle \mathscr{N}_0, 1\rangle] < \infty$*, then for all* $\tau \geq 0$*, a.s.*

$$\int_{\bar{\mathscr{D}}_G} \mathscr{N}_\tau(dx)\mathscr{N}_\tau(\{x\}) = \langle \mathscr{N}_\tau, 1\rangle, \tag{3.2}$$

that is $\sup_{x\in\bar{\mathscr{D}}_G} \mathscr{N}_\tau(\{x\}) \leq 1$.

Proof For all $\tau \geq 0$, let $\Phi(\mathscr{N}_\tau) = \int_{\bar{\mathscr{D}}_G} \mathscr{N}_\tau(dx)\mathscr{N}_\tau(\{x\}) - \langle \mathscr{N}_\tau, 1\rangle$. Note that the function Φ is nonnegative and a.s. $\Phi(\mathscr{N}_0) = 0$. Moreover, for any x in the support of the measure $\mathscr{N} \in \mathcal{M}_F(\bar{\mathscr{D}}_G)$, we have $\Phi(\mathscr{N}_\tau - \delta_x) - \Phi(\mathscr{N}_\tau) \leq 0$. For any $n \in \mathbb{N}^*$, we consider again the stopping time $\tau_n = \inf\{\tau \geq 0, \langle \mathscr{N}_\tau, 1\rangle \geq n\}$ and deduce from (2.8) that

$$\begin{aligned}\mathbb{E}[\Phi(\mathscr{N}_{\tau\wedge\tau_n})] \leq 0 &+ \alpha\mathbb{E}\Big[\int_0^{\tau\wedge\tau_n}\int_{\bar{\mathscr{D}}_G} \mathscr{N}_t(dx)\int_{\mathbb{R}^d}\Big\{\Phi(\mathscr{N}_t + \{\delta_{(x+z)}\}) - \Phi(\mathscr{N}_t)\Big\}K^{\mathsf{inv}}(x,dz)dt\Big] \\ &+ \mathbb{E}\Big[\int_0^{\tau\wedge\tau_n}\int_{\bar{\mathscr{D}}_G}\Big\{\int_{\bar{\mathscr{D}}_G}\big(\Phi(\mathscr{N}_t + \delta_{(y)}) - \Phi(\mathscr{N}_t)\big)\mathsf{aff}(x,y)K^{\mathsf{aff}}(dy)\Big\}\mathscr{N}_t(dx)dt\Big],\end{aligned}$$

where the first and the second terms of the right-hand side are equal to zero because $K^{\mathsf{inv}}(x,dz)$ and $K^{\mathsf{aff}}(dy)$ have densities together with the fact that $\mathscr{N}$ is atomic. We conclude that a.s. $\Phi(\mathscr{N}_{\tau\wedge\tau_n}) = 0$ and we finish the proof by remarking that $\tau_n \overset{n\to\infty}{\longrightarrow} \infty$ a.s. by using again (2.9) with $m = 1$. □

The next result shows the absolute continuity of the expectation of $\mathscr{N}_t$. We define the expectation of a random measure $\mathscr{N}$ by the deterministic measure $\mathbb{E}[\mathscr{N}]$ given by $\langle \mathbb{E}[\mathscr{N}], f\rangle = \mathbb{E}[\langle \mathscr{N}, f\rangle]$, for any measurable nonnegative function f.

Proposition 2 *Assume that assumptions (2.4) and (2.5) hold true, that* $\mathbb{E}[\langle \mathscr{N}_0, f\rangle] < \infty$ *and that* $\mathbb{E}[\mathscr{N}_0]$ *admits a density* $\tilde{g}_0$ *w.r.t. the Lebesgue measure. Then, for all* $\tau \geq 0$*,* $\mathbb{E}[\mathscr{N}_\tau]$ *has a density* $\tilde{g}_\tau$ *such that*

$$\mathbb{E}[\langle \mathscr{N}_\tau, f\rangle] = \int_{\bar{\mathscr{D}}_G} f(x)\tilde{g}_\tau(x)dx,$$

for all measurable nonnegative function f on $\bar{\mathscr{D}}_G$.

Proof Consider again, for any $n \in \mathbb{N}^*$, the stopping time τ_n. Let D be a Borel set of $\mathbb{R}^d$ with Lebesgue measure zero. Then we can write, by taking $\Phi(\mathscr{N}) = \langle \mathscr{N}, \mathbb{1}_D \rangle$ in (2.8) that, for all $\tau \geq 0$, all $n \geq 1$:

$$\begin{aligned}\mathbb{E}[\langle \mathscr{N}_{\tau\wedge\tau_n}, \mathbb{1}_D\rangle] = \mathbb{E}[\langle \mathscr{N}_0, \mathbb{1}_D\rangle] &+ \alpha\mathbb{E}\Big[\int_0^{\tau\wedge\tau_n}\int_{\bar{\mathscr{D}}_G} \mathscr{N}_t(dx)\int_{\mathbb{R}^d} \mathbb{1}_D(x+z)K^{\mathsf{inv}}(x,dz)dt\Big] \\ &- \beta\mathbb{E}\Big[\int_0^{\tau\wedge\tau_n}\int_{\bar{\mathscr{D}}_G} \mathscr{N}_t(dx)\mathbb{1}_D(x)dt\Big] \\ &+ A_{\mathsf{f}}\mathbb{E}\Big[\int_0^{\tau\wedge\tau_n}\int_{\bar{\mathscr{D}}_G}\Big\{\int_{\bar{\mathscr{D}}_G} \mathbb{1}_D(y)K^{\mathsf{aff}}(dy)\Big\}\mathscr{N}_t(dx)dt\Big].\end{aligned}$$

It is straightforward to check that the first term on the right-hand side vanishes since, by assumption, $\mathbb{E}[\langle \mathscr{N}_0, \mathbb{1}_D\rangle] = 0$. Moreover, for any $x \in \bar{\mathscr{D}}_G$, $\int_{\mathbb{R}^d} \mathbb{1}_D(x+z)K^{\mathsf{inv}}(x,dz) = 0$, then the second term is also zero. Furthermore, the third term is obviously nonpositive. Finally, the last term is zero since $\int_{\bar{\mathscr{D}}_G} \mathbb{1}_D(y)K^{\mathsf{aff}}(dy) = 0$. Therefore we deduce that, for any $n \in \mathbb{N}^*$, $\mathbb{E}[\langle \mathscr{N}_{\tau\wedge\tau_n}, \mathbb{1}_D\rangle]$ is nonpositive and thus zero. Hence, $\mathbb{E}[\mathscr{N}_{\tau\wedge\tau_n}]$ is absolutely continuous w.r.t. Lebesgue measure and thus, by the Radon-Nikodym theorem, there exists a measurable nonnegative function $\tilde{g}_{\tau\wedge\tau_n}$ such that $\langle \mathbb{E}[\mathscr{N}_{\tau\wedge\tau_n}], f\rangle = \int_{\bar{\mathscr{D}}_G} f(x)\tilde{g}_{\tau\wedge\tau_n}(x)dx$, for all $f \in C(\bar{\mathscr{D}}_G)$. To conclude, note again from (2.9) with $m = 1$ that a.s. $\tau_n \overset{n\to\infty}{\longrightarrow} \infty$, which completes the proof. □

Our goal now is to sketch the long-time behavior of the model (its extinction and survival properties). First, we refer the reader to Etheridge (2004) for more details about the techniques used to prove extinction and survival in some specific continuous processes. In addition, extinction and survival have been largely studied for the general class of processes with state space $\mathbb{N}$. Unfortunately, their techniques cannot be adapted to discontinuous processes as is the case here. We are only able to handle a proof, under the compactness assumption of the state space $\bar{\mathscr{D}}_G$, that shows that the process $(\mathscr{N}_\tau)_{\tau\geq 0}$ does a.s. not survive when $\alpha \leq \beta$. Before stating a result in this sense, at first step we need to show the following technical Lemma 1 that is useful to show at a second step Theorem 3.

Lemma 1 *Assume that $\bar{\mathscr{D}}_G$ is compact in $\mathbb{R}^d$ and there exists a constant $\upsilon > 0$ such that, for all $r \geq 1$ and all $(r+1)$-particles $x^1, \ldots, x^r, y \in \bar{\mathscr{D}}_G$, we have*

$$\sum_{i=1}^{r} \mathbb{1}_{\{\|x^i - y\| \leq a_{\mathsf{f}}\}} \leq \sum_{i=1}^{r}\sum_{\ell=1}^{\varkappa} \mathbb{1}_{\mathcal{C}_\ell}(x^i)\mathbb{1}_{\mathcal{C}_\ell}(y) + \upsilon, \tag{3.3}$$

where $\{\mathcal{C}_\ell,\ \ell = 1, \ldots, \varkappa\}$ is a family of disjoint cubes of $\mathbb{R}^d$ with side $a_{\mathsf{f}}/\sqrt{d}$ that we need to cover the state space $\bar{\mathscr{D}}_G$. Then, there exists a non decreasing function $\phi : \mathbb{R}_+ \mapsto \mathbb{R}_+$,

satisfying $\phi(0) > 0$ *and* $\lim_{x\to\infty}\phi(x) = \infty$ *such that the map* $\phi(x)$ *is linear on* $[0,\infty)$ *and for all* $\mathscr{N} \in \mathcal{M}_F(\bar{\mathscr{D}}_G)$

$$\langle \mathscr{N} \otimes K^{\mathsf{aff}}, \mathsf{aff}\rangle \leq \phi(\langle \mathscr{N}, 1\rangle). \tag{3.4}$$

Proof Let consider a family $\mathscr{C} = \{\mathcal{C}_\ell,\ \ell = 1,\ldots,\varkappa\}$ of disjoint cubes of $\mathbb{R}^d$ with side $a_{\mathsf{f}}/\sqrt{d}$. We cover the state space $\bar{\mathscr{D}}_G$ with the finite number $\varkappa$ of cubes where we note that for each l and each $x, y \in \mathcal{C}_\ell$, $\|x - y\| \leq a_{\mathsf{f}}$. Obviously we have y in some cube ℓ' ($y \in \mathcal{C}_{\ell'}$ for $\ell' \in \{1,\ldots,\varkappa\}$). For all $r \geq 1$ and all $x^1,\ldots,x^r, y \in \bar{\mathscr{D}}_G$ we have

$$\begin{aligned}
\int_{\bar{\mathscr{D}}_G} \sum_{i=1}^{r} \mathsf{aff}(x^i, y) K^{\mathsf{aff}}(dy) &\leq \int_{\bar{\mathscr{D}}_G} \sum_{i=1}^{r} A_{\mathsf{f}} \mathbb{1}_{\{\|x^i - y\| \leq a_{\mathsf{f}}\}} K^{\mathsf{aff}}(dy) \\
&\leq A_{\mathsf{f}} \int_{\bar{\mathscr{D}}_G} \sum_{i=1}^{r} \sum_{\ell=1}^{\varkappa} \mathbb{1}_{\mathcal{C}_\ell}(x^i) \mathbb{1}_{\mathcal{C}_\ell}(y) K^{\mathsf{aff}}(dy) + A_{\mathsf{f}} \upsilon \\
&= A_{\mathsf{f}} \sum_{i=1}^{r} \mathbb{1}_{\mathcal{C}_{\ell'}}(x^i) \int_{\bar{\mathscr{D}}_G} \mathbb{1}_{\mathcal{C}_{\ell'}}(y) K^{\mathsf{aff}}(dy) + A_{\mathsf{f}} \upsilon \\
&\leq A_{\mathsf{f}} r \int_{\mathcal{C}_{\ell'}} K^{\mathsf{aff}}(dy) + A_{\mathsf{f}} \upsilon \\
&= A_{\mathsf{f}} r \mathbb{P}(y \in \mathcal{C}_{\ell'}) + A_{\mathsf{f}} \upsilon.
\end{aligned}$$

Now, since the process $\mathscr{N} \in \mathcal{M}_F(\bar{\mathscr{D}}_G)$ is atomic, we conclude that $\langle \mathscr{N} \otimes K^{\mathsf{aff}}, \mathsf{aff}\rangle \leq A_{\mathsf{f}} p_{\ell'} \langle \mathscr{N}, 1\rangle + A_{\mathsf{f}} \upsilon$ where $p_{\ell'} = \mathbb{P}(y \in \mathcal{C}_{\ell'})$ (for instance $p_{\ell'} = 1/\varkappa$ if the affinity kernel K^{aff} is uniformly distributed). Hence, immediately (3.4) holds with $\phi(r) = r A_{\mathsf{f}} p_{\ell'} + A_{\mathsf{f}} \upsilon$. □

Now, we are in position to demonstrate the following Theorem 3 about the long-time behavior of the empirical measure (2.1) on graphs.

Theorem 3 *Assume that conditions (2.4) and (2.5) are satisfied together with* $\mathbb{E}[\langle \mathscr{N}_0, 1\rangle] < \infty$. *Furthermore, admit that all the assumptions of Lemma 1 hold and assume also that* $\alpha \leq \beta$, *then the extinction time* $\tau_0^\star$ *is a.s. finite which says that*

$$\tau_0^\star = \inf\{\tau :\ \langle \mathscr{N}_\tau, 1\rangle = 0\} < \infty. \tag{3.5}$$

Proof Let us take $\Phi(\mathscr{N}) = \langle \mathscr{N}, 1\rangle$ in (2.8) (by setting $f = 1$ and $F(x) = x$). Writing

$$\begin{aligned}
\mathbb{E}[\langle \mathscr{N}_\tau, 1\rangle] &= \mathbb{E}[\langle \mathscr{N}_0, 1\rangle] + \alpha \mathbb{E}\Big[\int_0^\tau \int_{\bar{\mathscr{D}}_G} \mathscr{N}_t(dx) \int_{\mathbb{R}^d} K^{\mathsf{inv}}(x, dz) dt\Big] \\
&\quad - \beta \mathbb{E}\Big[\int_0^\tau \int_{\bar{\mathscr{D}}_G} \mathscr{N}_t(dx) dt\Big] \\
&\quad + \mathbb{E}\Big[\int_0^\tau \int_{\bar{\mathscr{D}}_G} \Big\{\int_{\bar{\mathscr{D}}_G} \mathsf{aff}(x, y) K^{\mathsf{aff}}(dy)\Big\} \mathscr{N}_t(dx) dt\Big] \\
&= \mathbb{E}[\langle \mathscr{N}_0, 1\rangle] + \int_0^\tau \mathbb{E}\Big[\langle \mathscr{N}_t, \alpha - \beta\rangle\Big] dt \\
&\quad + \int_0^\tau \mathbb{E}\Big[\int_{\bar{\mathscr{D}}_G} \Big\{\int_{\bar{\mathscr{D}}_G} \mathsf{aff}(x, y) K^{\mathsf{aff}}(dy)\Big\} \mathscr{N}_t(dx)\Big] dt.
\end{aligned}$$

Now, since $\mathbb{E}[\langle \mathscr{N}_\tau, 1\rangle]$ is differentiable, by differentiating $\mathbb{E}[\langle \mathscr{N}_\tau, 1\rangle]$ we obtain

$$\begin{aligned}
\partial_\tau \mathbb{E}[\langle \mathscr{N}_\tau, 1\rangle] &= (\alpha - \beta)\mathbb{E}[\langle \mathscr{N}_\tau, 1\rangle] + \mathbb{E}[\langle \mathscr{N}_\tau \otimes K^{\mathsf{aff}}, \mathsf{aff}\rangle] \\
&\leq (\alpha - \beta)\mathbb{E}[\langle \mathscr{N}_\tau, 1\rangle] + \mathbb{E}[\phi(\langle \mathscr{N}_\tau, 1\rangle)] \qquad (3.6) \\
&= (\alpha - \beta)\mathbb{E}[\langle \mathscr{N}_\tau, 1\rangle] + \phi(\mathbb{E}[\langle \mathscr{N}_\tau, 1\rangle]), \qquad (3.7)
\end{aligned}$$

where inequality (3.6) is obtained from Lemma 1 and equality (3.7) holds by the fact that $\mathbb{E}[\phi(r)] = \phi(\mathbb{E}[r])$ (since ϕ is linear from $\mathbb{N}$ to $\mathbb{R}_+^*$). We know from Lemma 1 that the map $\phi(x)$ is nondecreasing and satisfying $\phi(0) > 0$ together with $\lim_{x\to\infty} \phi(x) = \infty$. By considering x_0 the greatest solution of $(\alpha - \beta)x_0 = -\phi(x_0)$ and by using (3.7) we obtain that, for all $\tau \geq 0$, $\mathbb{E}[\langle \mathscr{N}_\tau, 1\rangle] \leq \max(\mathbb{E}[\langle \mathscr{N}_0, 1\rangle], x_0)$. Hence, we deduce immediately that

$$\sup_{\tau \geq 0} \mathbb{E}[\langle \mathscr{N}_\tau, 1\rangle] < \infty. \qquad (3.8)$$

In the rest of the proof, we deal with the $\mathbb{N}$-valued process $N_\tau = \langle \mathscr{N}_\tau, 1\rangle$. Our main goal now is to check that, for any $n \in \mathbb{N}^*$, we have

$$\mathbb{P}(\liminf_{\tau\to\infty} \langle \mathscr{N}_\tau, 1\rangle = n) = 0. \qquad (3.9)$$

To verify (3.9), let us admit that $\liminf_{\tau\to\infty} \langle \mathscr{N}_\tau, 1\rangle = n$. Then clearly the size process $\langle \mathscr{N}_\tau, 1\rangle$ reaches infinitely often the state n and reaches a finite number of times the state $n-1$. Straightforwardly, this is a.s. impossible since each time $\langle \mathscr{N}_\tau, 1\rangle$ reaches the state n, the probability that its next state is $n-1$ is bounded from below by $(\beta/(\alpha + \beta + A_{\mathsf{f}})) > 0$.

Now, since $\langle \mathscr{N}_\tau, 1\rangle$ is $\mathbb{N}$-valued, we immediately conclude from (3.9) that a.s.

$$\liminf_{\tau\to\infty} \langle \mathscr{N}_\tau, 1\rangle \in \{0, \infty\}. \qquad (3.10)$$

Furthermore, since zero is an absorbing state, we deduce from (3.10) that a.s. $\lim_{\tau\to\infty}\langle\mathscr{N}_\tau,1\rangle$ exists and

$$\lim_{\tau\to\infty}\langle\mathscr{N}_\tau,1\rangle\in\{0,\infty\}. \tag{3.11}$$

By applying Fatou's lemma together with (3.8) we obtain

$$\mathbb{E}[\lim_{\tau\to\infty}\langle\mathscr{N}_\tau,1\rangle]=\mathbb{E}[\liminf_{\tau\to\infty}\langle\mathscr{N}_\tau,1\rangle]\leq\liminf_{\tau\to\infty}\mathbb{E}[\langle\mathscr{N}_\tau,1\rangle]\leq\sup_{\tau\geq0}\mathbb{E}[\langle\mathscr{N}_\tau,1\rangle]<\infty. \tag{3.12}$$

Hence a.s. $\lim_{\tau\to\infty}\langle\mathscr{N}_\tau,1\rangle<\infty$ and it's easily seen from (3.11) that a.s. $\lim_{\tau\to\infty}\langle\mathscr{N}_\tau,1\rangle=0$. This proves the theorem. □

Let us make some comments on the proof of this result now. Our main tool is a completely general requirement that the vertices degree be bounded in the sense of inequality (3.3) used to show Lemma 1 as well as the restriction $\alpha\leq\beta$ on the two rates of the system. Recall that the number of neighbors of a given vertex is the degree of the associated vertex. The existence of the positive constant υ in the right-hand side of (3.3) is trivial on any graph since the size of the system N and a_{f} are bounded above every time. The striking fact is that the order of magnitude of υ seems necessary to evaluate the extinction time: if vertices of larger and larger degree are present in the graph G, this should only contribute to the extinction time being larger. Still, one can study the dependence of the extinction time on the value of (υ,Λ) and this needs to be carried out in its own right. In the light of this result, the question of how the expectation of $\tau_0^\star$ grows with the number of vertices on finite graphs of degree bounded by a given number needs a much deeper investigation.

Remark 1 *More generally, let consider the process $(\mathscr{N}_\tau)_{\tau\geq0}$ with state dependent rates $\alpha(x)$ and $\beta(x)$. Assume that there exist some constants $\alpha\leq\beta$ such that for all $x\in\bar{\mathscr{D}}_G$, $\alpha(x)\leq\alpha$ and $\beta(x)\geq\beta$. Then $(\mathscr{N}_\tau)_{\tau\geq0}$ dies out a.s., meaning that for any finite initial configuration, the empty graph configuration is almost surely eventually reached, that is, $\mathbb{P}(\exists\tau>0,\langle\mathscr{N}_\tau,1\rangle=0)=1$.*

Remark 2 *In contrast, we can show that in some cases the process $(\mathscr{N}_\tau)_{\tau\geq0}$ survives with positive probability. At first glance, the problem is that the assumptions for the survival will never be mild (e.g. the space state $\bar{\mathscr{D}}_G$ will never be continuous or one needs to constrain the affinity function to be completely local; i.e., $\mathsf{aff}(x,y)=A_{\mathsf{f}}\mathbb{1}_{\{x=y\}}$) since we have to establish a rigorous coupling with the contact process. The task seems very difficult and much appropriate investigations are widely requested to be able to handle a proof in a general case.*

4 Nonparametric inference

In this section, we propose a spline nonparametric inference to approximate the distribution of a rescaled version of the system size process which assesses the extinction order of magnitude and its time evolution. Spline modeling for densities estimation has been used for instance by

Stone (1990) who shows that the sieved maximum likelihood estimator attains the optimal rate of convergence for estimating a smooth density. Our objective precisely consists in estimating a complicated distribution based on large sample over time. When we deal with the $\mathbb{N}$-valued process $N_\tau = \langle \mathscr{N}_\tau, 1 \rangle$, we may obtain a rescaled formulation of this size process, which will be the base of our study, by

$$S_\tau := \frac{\langle \mathscr{N}_\tau, 1 \rangle}{N^\star}, \qquad \tau \geq 0. \tag{4.1}$$

Here $N^\star > 0$ denotes the order of magnitude of the network size N_τ of interest and the rescaled process (4.1) is a $[0, \infty)$-valued pure jump process $(S_\tau)_{\tau \geq 0}$ (exactly with values in $\frac{1}{N^\star}\mathbb{N}$). This classical rescaled technique is chiefly employed in our context to study a normalized version from the initial discrete size process.

Because of the extinction in finite time (under the assumptions of Theorem 3), the distribution of the rescaled size process fails to have a density w.r.t. the Lebesgue measure on $[0, \infty)$. Roughly, let $P_\tau(dv|s) = \mathbb{P}(S_{t+\tau} \in dv | S_t = s)$ be the transition kernel of the process $(S_\tau)_{\tau \geq 0}$ and let $\pi_\tau(dv) = (\pi_0 P_\tau)(dv)$ be the distribution of S_τ where π_0 denotes the initial distribution. We need to explain the notation of the right action on measure by: $(\pi_0 P_\tau)(dv) = \int_{\mathbb{R}_+} \pi_0(ds) P_\tau(dv|s)$. The probability measure $P_\tau(\cdot|s)$ gives positive probability to zero the absorbing state and we may decompose it rigorously into singular part E_τ and absolutely continuous part p_τ from the following Lebesgue decomposition:

$$P_\tau(dv|s) = E_\tau(s)\delta_0(dv) + p_\tau(v|s)dv, \tag{4.2}$$

where δ_0 is the Dirac mass at state 0 and dv is the Lebesgue measure on $[0, \infty)$. Particularly, P_τ is absolutely continuous w.r.t. the reference measure $m(dv) = \delta_0(dv) + dv$ on $\mathbb{R}_+$ with density

$$p^\star_\tau(v|s) = \begin{cases} E_\tau(s), & \text{if } v = 0\,, \\ p_\tau(v|s), & \text{otherwise.} \end{cases} \tag{4.3}$$

To complete the presentation of the distribution under study, we suppose also that the initial distribution π_0 is absolutely continuous with respect to the reference measure $m(dv)$, and we let:

$$p^\star_0(v) = \frac{\pi_0(dv)}{m(dv)} = \begin{cases} E_0, & \text{if } v = 0\,, \\ p_0(v), & \text{otherwise.} \end{cases} \tag{4.4}$$

We assume that there are n observations $V_n^\tau = (v_{\tau_1}, \ldots, v_{\tau_n})$ sampled from an unknown distribution $P_\tau(\cdot|s)$ on the interval $[0, \infty)$ in the real line that is bounded away from infinity with $\tau \in (0, T]$. Our model on this measure will be supported on the set of smooth functions constructed from a spline basis. Fix some "order" q, a natural number such that $q \geq 3$, and let $L(\tau) \geq 2$ be another natural number, which will increase with n, and partition the half-open interval $[\min(V_n^\tau), \max(V_n^\tau))$ into $L(\tau)$ subintervals $[\min(V_n^\tau) + (l-1)\Delta_n^\tau / L(\tau), \min(V_n^\tau) + l\Delta_n^\tau / L(\tau))$ for $l = 1, \ldots, L(\tau)$ and $\Delta_n^\tau = \max(V_n^\tau) - \min(V_n^\tau)$. Consider the linear space of splines

of order q relative to this partition, that is, all functions $p : [0, \infty) \mapsto \mathbb{R}$ which are piecewise polynomial of degree $< q$ and which are $q - 2$ times continuously differentiable. This space of splines has dimension $J(\tau) = q + L(\tau) - 1$. The reader can find a thorough presentation of splines in de Boor (2001). We are tempted to use the set of M-splines $M_{1,q}, \ldots, M_{J(\tau),q}$ of order q and with the known nondecreasing sequence of knots $\xi_\tau = (\xi_1^\tau, \ldots, \xi_{L(\tau)-1+2q}^\tau)$. It is worthwhile to stress that the exact nature of M-spline function does not matter to us here, except that it refers to a certain normalized B-spline function on its minimal support $[\xi_j^\tau, \xi_{j+q}^\tau)$, i.e., $M_{j,q} := (q/(\xi_{j+q}^\tau - \xi_j^\tau))B_{j,q}$ which implies straightforwardly that $\int_{-\infty}^{+\infty} M_{j,q} = \int_{\xi_j^\tau}^{\xi_{j+q}^\tau} M_{j,q} = 1$.

The transition kernel $P_\tau(dv|s)$ is a probability measure for any $s \geq 0$, so that the extinction probability $E_\tau(s)$ starting from s satisfies, for all $\tau \in [0, T]$ and $s, v \in [0, \infty)$

$$\int_{\mathbb{R}_+} p_\tau(v|s)dv = 1 - E_\tau(s). \tag{4.5}$$

In practice, the issue is that the function $p_\tau(v|s)$ is not available in closed form. For $\theta_\tau \in \mathbb{R}_+^{J(\tau)}$ (to meet the requirement that p_τ needs to be positive since it is known that $M_{j,q} \geq 0$) let us approximate the continuous part with the spline:

$$p_\tau^\theta(v|s) = \sum_{j=1}^{J(\tau)} \theta_j^\tau M_{j,q}(v, \tau). \tag{4.6}$$

As a consequence of the preceding modeling, the problem of routine calculation of spline coefficients, that depend on the time, may be addressed using the maximization of the log-likelihood as follows:

$$(\hat{\theta}_1^\tau, \ldots, \hat{\theta}_{J(\tau)}^\tau) = \underset{(\theta_1^\tau, \ldots, \theta_{J(\tau)}^\tau) \in \Theta(\tau)}{\arg\max} \mathscr{L}(v_{\tau_1}, \ldots, v_{\tau_n}, \theta_\tau), \tag{4.7}$$

where the log-likelihood that takes into account the extinction is given by

$$\mathscr{L}(v_{\tau_1}, \ldots, v_{\tau_n}, \theta_\tau) = \sum_{k=1}^{n} \log\Big(E_\tau(s) + \sum_{j=1}^{J(\tau)} \theta_j^\tau M_{j,q}(v_{\tau_k}, \tau)\Big), \tag{4.8}$$

and we could restrict θ_τ to the subset

$$\Theta(\tau) = \Big\{\theta_\tau \in \mathbb{R}_+^{J(\tau)} : \sum_{j=1}^{J(\tau)} \theta_j^\tau \int_{\mathbb{R}_+} M_{j,q}(v, \tau)dv = 1 - E_\tau(s)\Big\}. \tag{4.9}$$

Note that, in (4.8), the irrelevant density of the initial observation, S_0, has been left out since n will be chosen large. Hence the equation (4.7) defines a nonlinear programming problem. In the following we construct a solution to this problem (that may vary over time and extinction level) for the set of probability densities on $[0, \infty)$, which next induces a nonparametric model on the continuous part of probability densities p_τ^θ through the map $\theta_\tau \mapsto p_\tau^\theta$.

Theorem 4 *The problem defined by equation (4.7) has a unique solution on $\Theta(\tau)$. Suppose that $\hat{\theta}_\tau = (\hat{\theta}_1^\tau, \ldots, \hat{\theta}_{J(\tau)}^\tau)$ is a solution to the maximization of the log-likelihood (4.8) on the constrained subset (4.9), then, for $j = 1, \ldots, J(\tau)$, it must satisfy*

$$\hat{\theta}_j^\tau = \frac{\big(1 - E_\tau(s)\big) \sum_{k=1}^n \frac{\hat{\theta}_j^\tau M_{j,q}(v_{\tau_k}, \tau)}{E_\tau(s) + \sum_{j=1}^{J(\tau)} \hat{\theta}_j^\tau M_{j,q}(v_{\tau_k}, \tau)}}{\Big(n - \sum_{k=1}^n \frac{E_\tau(s)}{E_\tau(s) + \sum_{j=1}^{J(\tau)} \hat{\theta}_j^\tau M_{j,q}(v_{\tau_k}, \tau)}\Big) \int_{\mathbb{R}_+} M_{j,q}(v, \tau) dv}. \tag{4.10}$$

Proof From Weierstrass' theorem, which states that a continuous function defined on a compact interval must have an extreme, we conclude that the solution to maximization (4.7) exists. Writing the Lagrangian in the following form:

$$\mathcal{L} = \sum_{k=1}^n \log \Big\{ E_\tau(s) + \sum_{j=1}^{J(\tau)} \theta_j^\tau M_{j,q}(v_{\tau_k}, \tau) \Big\} + \lambda \Big\{ \sum_{j=1}^{J(\tau)} \theta_j^\tau \int_{\mathbb{R}_+} M_{j,q}(v, \tau) dv - (1 - E_\tau(s)) \Big\}. \tag{4.11}$$

The derivatives of $\mathcal{L}$ with respect to θ_τ are, for $j = 1, \ldots, J(\tau)$

$$\frac{\partial \mathcal{L}}{\partial \theta_j^\tau} = \sum_{k=1}^n \frac{M_{j,q}(v_{\tau_k}, \tau)}{E_\tau(s) + \sum_{j=1}^{J(\tau)} \theta_j^\tau M_{j,q}(v_{\tau_k}, \tau)} + \lambda \int_{\mathbb{R}_+} M_{j,q}(v, \tau) dv. \tag{4.12}$$

Let $\hat{\theta}_\tau$ be an optimum that satisfies

$$\hat{\theta}_j^\tau \Big(\frac{\partial \mathcal{L}}{\partial \theta_j^\tau}\Big|_{\theta_j^\tau = \hat{\theta}_j^\tau} \Big) = \sum_{k=1}^n \frac{\hat{\theta}_j^\tau M_{j,q}(v_{\tau_k}, \tau)}{E_\tau(s) + \sum_{j=1}^{J(\tau)} \hat{\theta}_j^\tau M_{j,q}(v_{\tau_k}, \tau)} + \lambda \hat{\theta}_j^\tau \int_{\mathbb{R}_+} M_{j,q}(v, \tau) dv = 0. \tag{4.13}$$

Summing up the above equations over j and exchanging the order of summation signs lead to

$$\begin{aligned} \sum_{j=1}^J \hat{\theta}_j^\tau \Big(\frac{\partial \mathcal{L}}{\partial \theta_j^\tau}\Big|_{\theta_j^\tau = \hat{\theta}_j^\tau} \Big) &= \sum_{j=1}^{J(\tau)} \sum_{k=1}^n \frac{\hat{\theta}_j^\tau M_{j,q}(v_{\tau_k}, \tau)}{E_\tau(s) + \sum_{j=1}^{J(\tau)} \hat{\theta}_j^\tau M_{j,q}(v_{\tau_k}, \tau)} + \lambda \sum_{j=1}^{J(\tau)} \hat{\theta}_j^\tau \int_{\mathbb{R}_+} M_{j,q}(v, \tau) dv \qquad (4.14) \\ &= \sum_{k=1}^n \frac{\sum_{j=1}^{J(\tau)} \hat{\theta}_j^\tau M_{j,q}(v_{\tau_k}, \tau)}{E_\tau(s) + \sum_{j=1}^{J(\tau)} \hat{\theta}_j^\tau M_{j,q}(v_{\tau_k}, \tau)} + \lambda \sum_{j=1}^{J(\tau)} \hat{\theta}_j^\tau \int_{\mathbb{R}_+} M_{j,q}(v, \tau) dv = 0, \end{aligned}$$

where in (4.14) the denominator of the first term is independent on the index j which justifies that the summation is performed only on the numerator. The sum in the second term is $(1 - E_\tau(s))$ on the subset $\Theta(\tau)$. Thus we obtain

$$\begin{aligned} \sum_{j=1}^{J(\tau)} \hat{\theta}_j^\tau \Big(\frac{\partial \mathcal{L}}{\partial \theta_j^\tau}\Big|_{\theta_j^\tau = \hat{\theta}_j^\tau} \Big) &= \sum_{k=1}^n \Big\{ 1 + \frac{-E_\tau(s)}{E_\tau(s) + \sum_{j=1}^{J(\tau)} \hat{\theta}_j^\tau M_{j,q}(v_{\tau_k}, \tau)} \Big\} + \lambda(1 - E_\tau(s)) \\ &= n - \sum_{k=1}^n \frac{E_\tau(s)}{E_\tau(s) + \sum_{j=1}^{J(\tau)} \hat{\theta}_j^\tau M_{j,q}(v_{\tau_k}, \tau)} + \lambda(1 - E_\tau(s)) = 0. \end{aligned}$$

From the last equation we are led to deduce the Lagrange multiplier, which satisfies the Kuhn-Tucker conditions:

$$\lambda = \frac{-n + \sum_{k=1}^{n} \frac{E_\tau(s)}{E_\tau(s)+\sum_{j=1}^{J(\tau)} \hat{\theta}_j^\tau M_{j,q}(v_{\tau_k},\tau)}}{(1 - E_\tau(s))}. \tag{4.15}$$

Substituting (4.15) into equation (4.13), we have

$$\sum_{k=1}^{n} \frac{\hat{\theta}_j^\tau M_{j,q}(v_{\tau_k},\tau)}{E_\tau(s) + \sum_{j=1}^{J(\tau)} \hat{\theta}_j^\tau M_{j,q}(v_{\tau_k},\tau)} + \hat{\theta}_j^\tau \Big(\frac{-n + \sum_{k=1}^{n} \frac{E_\tau(s)}{E_\tau(s)+\sum_{j=1}^{J(\tau)} \hat{\theta}_j^\tau M_{j,q}(v_{\tau_k},\tau)}}{(1 - E_\tau(s))} \Big) \int_{\mathbb{R}_+} M_{j,q}(v,\tau) dv = 0.$$

This gives the iteration formula (4.10). Now, we shall show the uniqueness of the solution, that is there exists only one extreme point interior to $\Theta(\tau)$ for this nonlinear problem. Roughly, we will prove that if $\hat{\theta}_\tau$ is an optimum solution, it must be the global optimum. By direct calculation and Taylor's theorem, we have:

$$\begin{aligned}
\mathcal{L}(\theta_\tau) &\approx \mathcal{L}(\hat{\theta}_\tau) + \sum_{j=1}^{J(\tau)} \Big(\frac{\partial \mathcal{L}(\hat{\theta}_\tau)}{\partial \theta_j^\tau} \Big) (\theta_j^\tau - \hat{\theta}_j^\tau) + \frac{1}{2} \sum_{j=1}^{J(\tau)} \sum_{j'=1}^{J(\tau)} \Big(\frac{\partial^2 \mathcal{L}(\tilde{\theta}_\tau)}{\partial \theta_j^\tau \partial \theta_{j'}^\tau} \Big) (\theta_j^\tau - \hat{\theta}_j^\tau)(\theta_{j'}^\tau - \hat{\theta}_{j'}^\tau) \\
&= \mathcal{L}(\hat{\theta}_\tau) + \sum_{j=1}^{J(\tau)} \Big(\frac{\partial \mathcal{L}(\hat{\theta}_\tau)}{\partial \theta_j^\tau} \Big) (\theta_j^\tau - \hat{\theta}_j^\tau) - \frac{1}{2} \sum_{j=1}^{J(\tau)} \sum_{j'=1}^{J(\tau)} \sum_{k=1}^{n} \frac{M_{j,q}(v_{\tau_k},\tau) M_{j',q}(v_{\tau_k},\tau)(\theta_j^\tau - \hat{\theta}_j^\tau)(\theta_{j'}^\tau - \hat{\theta}_{j'}^\tau)}{\big(E_\tau(s) + \sum_{j=1}^{J(\tau)} \tilde{\theta}_j^\tau M_{j,q}(v_{\tau_k},\tau)\big)^2} \\
&= \mathcal{L}(\hat{\theta}_\tau) + \sum_{j=1}^{J(\tau)} \Big(\frac{\partial \mathcal{L}(\hat{\theta}_\tau)}{\partial \theta_j^\tau} \Big) (\theta_j^\tau - \hat{\theta}_j^\tau) - \frac{1}{2} \sum_{k=1}^{n} \frac{\Big(\sum_{j=1}^{J(\tau)} (\theta_j^\tau - \hat{\theta}_j^\tau) M_{j,q}(v_{\tau_k},\tau) \Big)^2}{\big(E_\tau(s) + \sum_{j=1}^{J(\tau)} \tilde{\theta}_j^\tau M_{j,q}(v_{\tau_k},\tau)\big)^2},
\end{aligned}$$

for $\tilde{\theta}_\tau$ a vector on the line segment between θ_τ and $\hat{\theta}_\tau$. It's easily seen that the third term on the right hand side of the last equation is less than zero. We can finish the proof by concluding that

$$\mathcal{L}(\theta_\tau) \leq \mathcal{L}(\hat{\theta}_\tau) + \sum_{j=1}^{J(\tau)} \Big(\frac{\partial \mathcal{L}(\hat{\theta}_\tau)}{\partial \theta_j^\tau} \Big) (\theta_j^\tau - \hat{\theta}_j^\tau). \tag{4.16}$$

As known, (4.16) is the sufficient condition for $\hat{\theta}_\tau \in \Theta(\tau)$ to be the global maximum [see, for example, Luenberger & Ye (2016)]. It follows that the necessary conditions are satisfied easily and this concludes the proof. □

Although in this section we are primarily interested in smooth continuous part of the transition kernel modeling for the rescaled size process, it is desirable to have a unified methodology applicable to network size distributions that does contain the atomless (has no atom at 0) continuous probability measures which are not absolutely continuous. Let us now consider some simply functions (in Figures 2 and 3) picked up for illustrative purposes. An example of such a measure

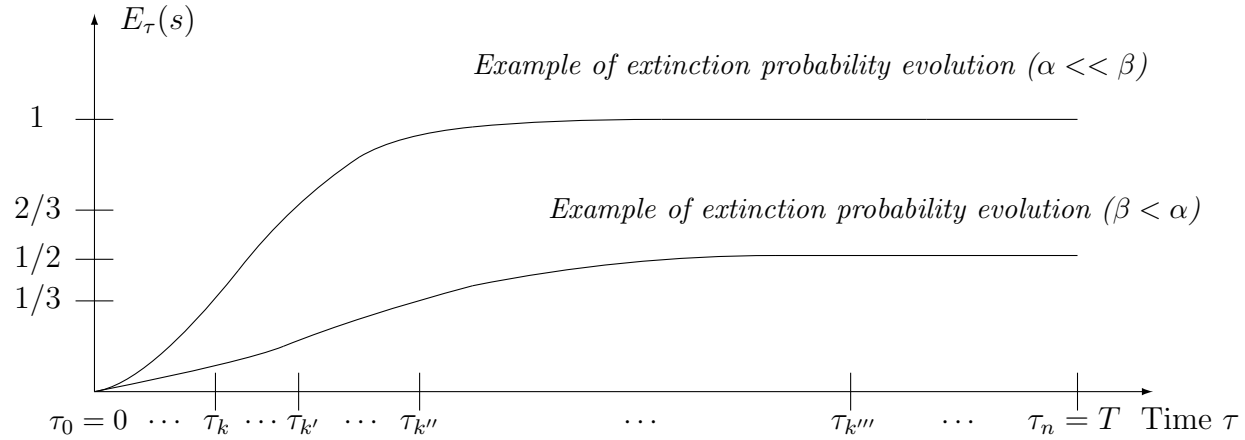

Figure 2: Two examples of extinction probability evolution. The process parameter values are chosen so as to observe a short transient phase where the rescaled network size grows quickly, starting from a small initial size value, and reaches a stationary phase in the short term $[0, T]$.

may be observed in some cases, for instance, when $\alpha >> \beta$. For an order $q = 1$ the linear space of splines consists of piecewise constant functions with cell boundaries $(\min(V_n^\tau) + l\Delta_n^\tau / L(\tau))$ for $l = 0, 1, \ldots, L(\tau)$. The design of a spline model on the probability measure by considering $P_\tau \equiv \sum_{j=1}^{J(\tau)} \theta_j^\tau M_{j,1}$ enables us to approximate arbitrarily closely (when $L(\tau) \uparrow \infty$) this class of measures constructed on piecewise constant functions as a special case. Therefore, this class of discrete probability measures with atoms at $\{\min(V_n^\tau), \min(V_n^\tau) + \Delta_n^\tau / L(\tau), \ldots, \max(V_n^\tau)\}$ is weakly dense in the set of all probability measures $P_\tau(\cdot|s)$.

We conclude this section with some behavior examples of extinction probability and absolutely continuous mass evolution in the presence of the phenomenon of extinction. We assume first $\alpha << \beta$ to accelerate the extinction of the network and second $\beta < \alpha$ to highlight the possible presence of extinction even when assumption $\alpha \leq \beta$ of Theorem 3 is not meet. These examples of functions $E_\tau(s)$ and $p_\tau^\theta(v|s)$ are illustrated respectively in Figures 2 and 3.

Particularly, let us roughly specify the main ideas summarized in Figures 2 and 3. If we consider a high extinction level (case $\alpha << \beta$) a lot of withdrawal events occur just after the initial state, then during the transient phase of the size network process we expect a large amount of probability mass to be lost (in the continuous part of the measure) which quickly drives the network to extinction. More importantly, when the invitation rate is above the withdrawal rate we will show in Section 5 that the phenomenon of extinction is still present even in the short term. Moreover, on a large time scale the probability mass in the continuous part keeps on decreasing slowly, although the latter fact is not clearly diagnosed now (in case $\beta < \alpha$). The time behavior of the absolutely continuous part is then plotted at particular instants τ_k, $\tau_{k'}$, $\tau_{k''}$ and $\tau_{k'''}$ on Figure 3. By considering the case $\alpha << \beta$, the functions p_{τ_k} and $p_{\tau_k'}$ take high values near absorbing point 0. This induces a probability flow towards 0 and increases the extinction probability. In the second case $\beta < \alpha$, the functions $p_{\tau_k''}$ and $p_{\tau_k'''}$ show that the probability mass near the frontier point 0 is low since the extinction probability grows much more slowly within

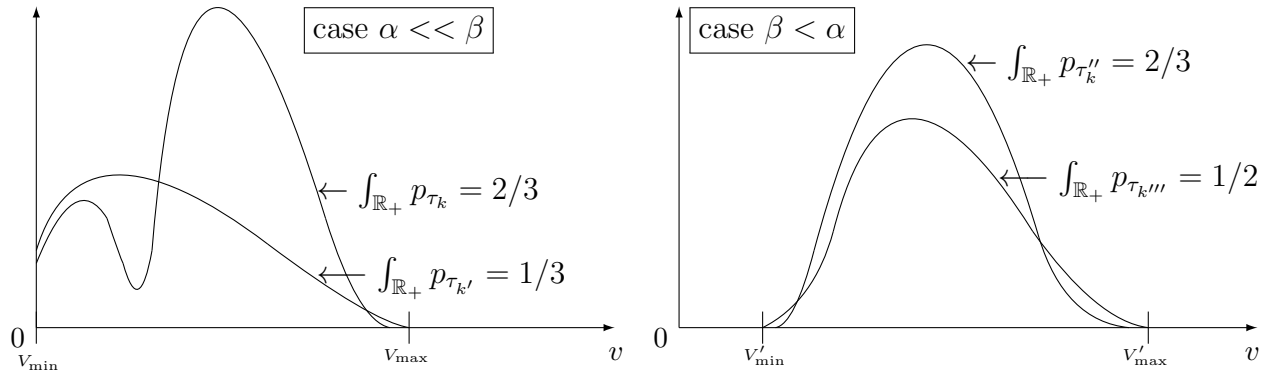

Figure 3: Examples of time evolution (at instants $\tau_k, \tau'_k, \tau''_k$ and τ'''_k marked in Figure 2) of the rescaled size distribution (absolutely continuous part). Extinction induces a quick loss of probability mass in the transient phase when $\alpha << \beta$. The loss of probability mass is then much slower when $\beta < \alpha$. Here, $V_{\min} = \min(V^\tau_k, V^\tau_{k'}), V_{\max} = \max(V^\tau_k, V^\tau_{k'}), V'_{\min} = \min(V^\tau_{k''}, V^\tau_{k'''})$ and $V'_{\max} = \max(V^\tau_{k''}, V^\tau_{k'''})$.

the time evolution.

5 Some numerical evidence

In this section, we present some short numerical results to illustrate the model and the main result about the long-time behavior that we discussed in this paper.

We stress first that random graphs on the space state cross time can be very conveniently generated thanks to the exact Monte Carlo scheme given by Algorithm 1. For this, we simulate some examples of dynamics since initial networks through continuous time. For simplicity, we shall illustrate these states in the unit square $[0,1]^2$. Then, each member of the network is characterized by a vertex with two coordinates inside the square. We let the algorithm run three times for the same number of iterations (10^5 updates) starting from the state $\mathscr{N}_0 \sim U_{[0,1]^2}$ with initial size $N_0 = 1000$ (see Figure 4). We run the algorithm with $\alpha = 3$, $\beta = 1.6$, $A_{\mathsf{f}} = 2$, $a_{\mathsf{f}} = 0.1$ and two Gaussian kernels (for invitation and affinity recruitments) with some dispersion parameter $\sigma > 0$. Figures 5, 6 and 7 show the final states with their degree distributions of the three simulated dynamics (with $\sigma = 0.001$, $\sigma = 0.005$ and $\sigma = 0.1$) starting from the initial state $\mathscr{N}_0$. We report this first numerical experiment to highlight the behavior of the network dynamics in function of the dispersion. Thus, we are interested in the influence of spatial dispersion on the formation of patterns (communities) and other aspects seen in real-world social network dynamics. The analysis of Figures 5, 6 and 7 shows that with high dispersion new vertices tend to occupy almost all the space and their dispersion is uniformly in the vicinity of already present vertices. With low dispersion new nodes tend to occupy only the space located in the vicinity of nodes that contributed to their recruitments. This favors the formation of clusters. Unsurprisingly with very small dispersion ($\sigma = 0.001$), the network dynamic evolves

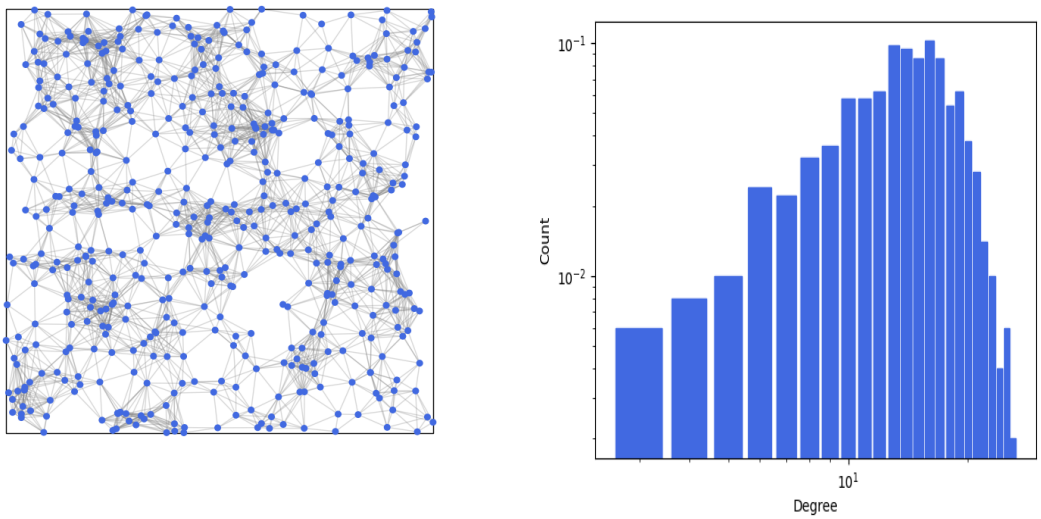

(a) Initial network state with $N_0 = 1000$ (b) Initial degree distribution

Figure 4: Initial network state and its initial degree distribution.

again through a process of clustering. On the basis of this numerical evidence, it appears that the impact of the dispersion level is important. We refer the interested reader, in this context, to Ugander et al. (2011) for some details about the anatomy of the facebook social graph.

We can now focus quickly on the main result of our paper, dealing with the large time behavior of the network. We perform simulations at different levels of extinction. To this end we vary the invitation and withdrawal rates. We consider three cases:

- small extinction (with $\alpha > \beta$): $\alpha = 2$, $\beta = 1.98$, $A_{\mathsf{f}} = 2.55$, $a_{\mathsf{f}} = 0.05$, $\sigma = 0.01$ and $N_0 = 100$,
- medium extinction (with $\alpha < \beta$): $\alpha = 2$, $\beta = 2.005$, $A_{\mathsf{f}} = 2.55$, $a_{\mathsf{f}} = 0.05$, $\sigma = 0.01$ and $N_0 = 100$,
- high extinction (with $\alpha < \beta$): $\alpha = 2$, $\beta = 2.015$, $A_{\mathsf{f}} = 2.55$, $a_{\mathsf{f}} = 0.05$, $\sigma = 0.01$ and $N_0 = 100$.

In each of these three cases, and with the same initial distribution, we simulate 60 independent runs of the network process using the scheme detailed in Algorithm 1 with 10^5 and 10^6 updates.

The evolution of the network sizes is illustrated through trajectories in Figure 8. In the figure, we report the realization of the network size for somewhat long periods, simply for illustrative purposes. It is easily seen from Figure 9 that, for the three extinction levels, the estimated extinction probability grows quickly in the first period, and seems to approach an asymptotic

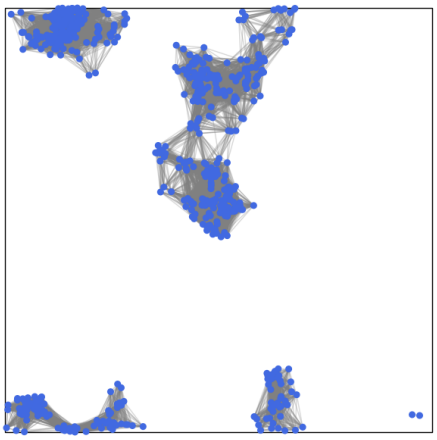

(a) Final network state (low dispersion)

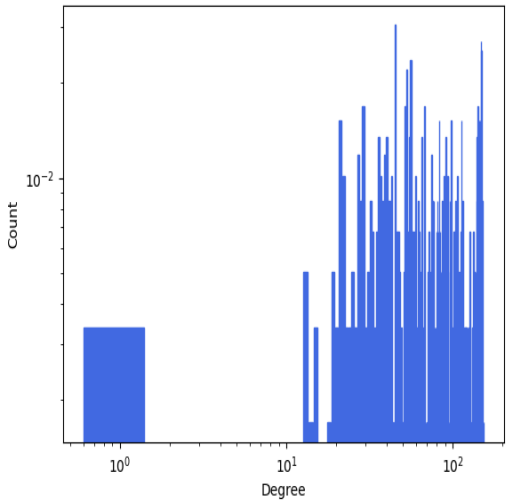

(b) Final degree distribution (low dispersion)

Figure 5: Final network state with dispersion $\sigma = 0.001$ and its degree distribution.

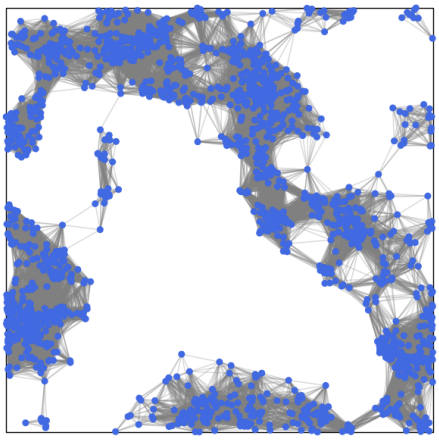

(a) Final network state (medium dispersion)

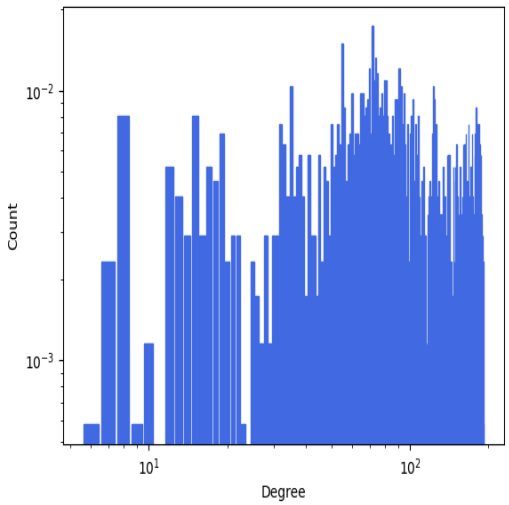

(b) Final degree distribution (medium dispersion)

Figure 6: Final network state with dispersion $\sigma = 0.005$ and its degree distribution.

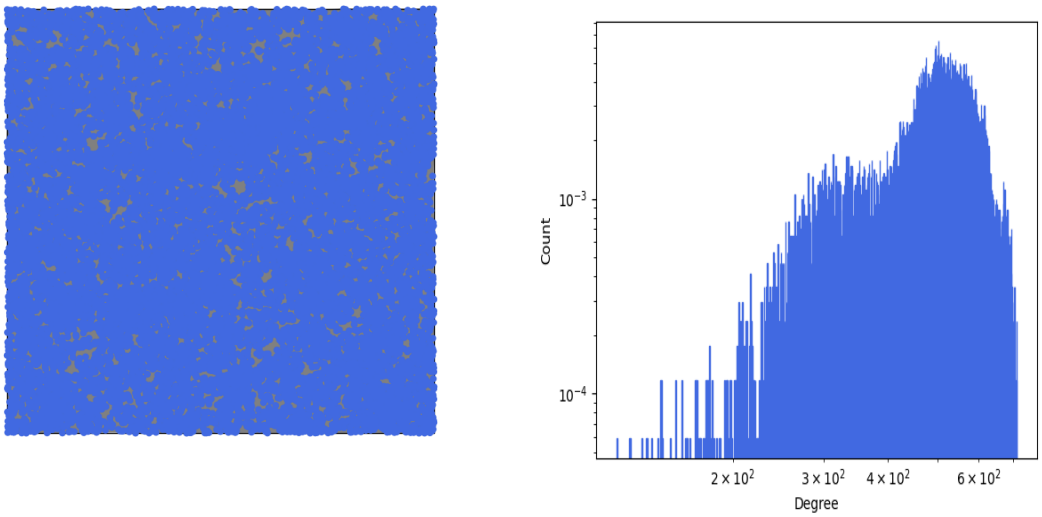

(a) Final network state (high dispersion) (b) Final degree distribution (high dispersion)

Figure 7: Final state of the network with dispersion $\sigma = 0.1$ and its degree distribution.

value. Running the simulation on a much larger period of time (more than 10^6 updates here) will result in an extinction probability growing to 1 at least almost surely in the cases with $\alpha \leq \beta$.

To extract a random sample $V_n^\tau = (v_{\tau_1}, \ldots, v_{\tau_n})$ from these trajectories to study its unknown distribution for each level of extinction we proceed as follows. Let us denote by n_τ^0 the number of trajectories that become extinct before instant τ from the total number of trajectories $n^\star = 60$. The probability of extinction is approximated at each time $\tau \in [0, T]$ by

$$E_\tau(s) = \frac{\text{Number of trajectories that extinct before instant } \tau}{\text{Total number of trajectories simulated by Monte Carlo}} = \frac{n_\tau^0}{n^\star}.$$

When we run 10^5 updates, this computation gives $E_T(s) = 7/60$ (in small extinction), $E_T(s) = 36/60$ (in medium extinction) and $E_T(s) = 55/60$ (in high extinction). With 10^6 updates, we obtain $E_T(s) = 7/60$ (in small extinction), $E_T(s) = 43/60$ (in medium extinction) and $E_T(s) = 58/60$ (in high extinction). Now, we can discretize all the simulated trajectories by setting a time step $\Delta^\star$ (a mesh) and computing the mean at each time step from the $n^\star$ values of the rescaled network size ($s_\tau^\ell = N_\tau^\ell / N^\star$, for $\ell = 1, \ldots, n^\star$). Then, we obtain a sample, which reads

$$(v_{\tau_1}, v_{\tau_2}, \ldots, v_{\tau_n}) = \left(\frac{\sum_{\ell=1}^{n^\star} s_{\Delta^\star}^\ell}{n^\star}, \frac{\sum_{\ell=1}^{n^\star} s_{2\Delta^\star}^\ell}{n^\star}, \ldots, \frac{\sum_{\ell=1}^{n^\star} s_{n\Delta^\star}^\ell}{n^\star} \right)$$

where the instants of discretization are clearly $\tau_1, \tau_2, \ldots, \tau_n = \Delta^\star, 2\Delta^\star, \ldots, n\Delta^\star$. In particular, in this numerical study we took $N^\star = N_0$.

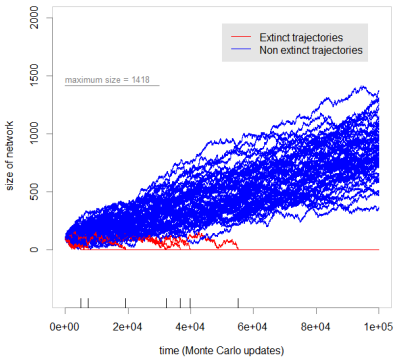

(a) Low extinction $E_T(s) = 0.1166667$ and 10^5 updates

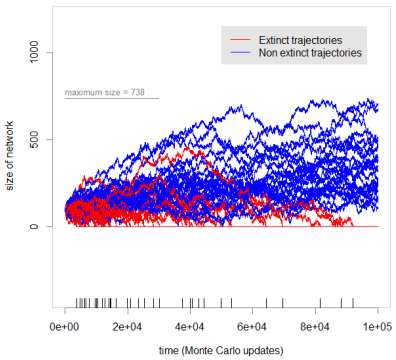

(b) Moderate extinction $E_T(s) = 0.6$ and 10^5 updates

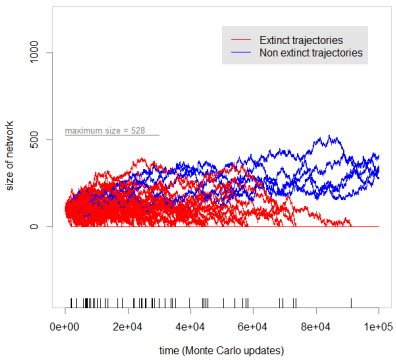

(c) High extinction $E_T(s) = 0.9166667$ and 10^5 updates

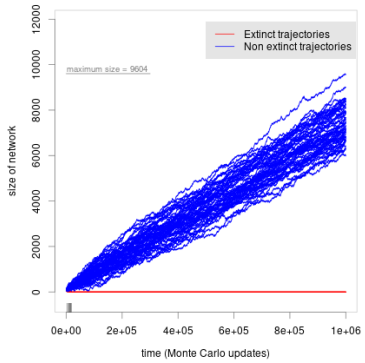

(d) Low extinction $E_T(s) = 0.1166667$ and 10^6 updates

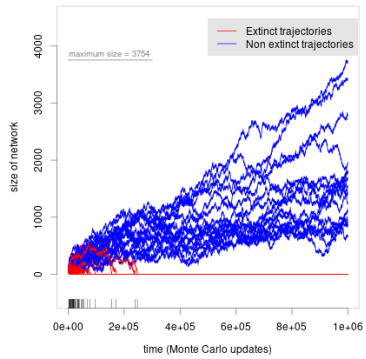

(e) Moderate extinction $E_T(s) = 0.7166667$ and 10^6 updates

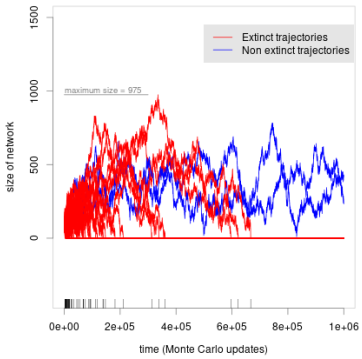

(f) High extinction $E_T(s) = 0.9666667$ and 10^6 updates

Figure 8: Sample trajectories that show the time evolution of the number of nodes during 10^5 updates (top) and 10^6 updates (bottom) for small, medium and large extinction levels for the network model. The instants of extinction for trajectories that extinct are indicated by the vertical stripes on the time-axis.

We are now in the position to use simulations to validate the previous results. For the computation of the spline that models the absolutely continuous part of the unknown density for the three levels of extinction, it is desirable to use our previous formula derived in (4.10) to find the spline coefficients in an iterative efficient way. We implemented a simple routine in R that is extremely efficient and allows to compute all the coefficients in a matter of seconds on a standard laptop computer. This is very promising since the coefficients have themselves a temporal dependence structure and we need to recompute the spline at each time. As common in the optimization context, we start the spline coefficients by a visual examination (from the histogram of the rescaled process data) when computing our estimators by (4.10), in order to avoid initialization issues. In all cases numerical tests have shown that it reaches in a fast manner the optimum which ensures that this formula is very computationally efficient even in high dimension (large n and large number of knots). In our case, however, we need to determine the optimal number of knots in the computation of the spline. The major advantages of the knot selection are its flexibility achieved by adjusting the spline to detect better the high and low variability regions of the data and to facilitate the control of the absolutely continuous part of the distribution. For this reason, we implemented a simple routine in R, to select the smallest knot sequence that gives the best "bias" at $\tau = T$:

$$B^{\star}(\xi_{\tau}) = \Big(\int_{\mathbb{R}_+} \sum_{j=1}^{J(\tau)} \theta_j^{\tau} M_{j,q}(v,\tau) dv - (1 - E_{\tau}(s)) \Big). \tag{5.1}$$

In Figure 10, we report the obtained spline curve at each case to illustrate the approximation one obtains by using the spline coefficients summarised, for completeness, in Table 1 and Table 2. We note how the estimators perform very efficiently, and show also in Figure 10 the "wrong histogram" (with area equal to 1) of the rescaled process to highlight the impact of the extinction on the loss of probability mass during the time evolution. In all cases, the average of the bias computed by (5.1) scales approximately as 10^{-4} to 10^{-6}.

Finally, we show in Figure 11 an example of dynamics without observing the extinction phenomenon for 10^6 updates. To obtain this scenario we took $\alpha = 2$, $\beta = 1.9$, $A_{\mathsf{f}} = 2.55$, $a_{\mathsf{f}} = 0.05$, $\sigma = 0.01$ and $N_0 = 100$.

Clearly, a full assessment of the long-time behavior would require much deeper theoretical and numerical investigations; these preliminary results, however, seem rather encouraging for future developments to assess an extinction threshold (a critical value of β that ensures the extinction of the network).

References

Aldous D. (1997). Brownian excursions, critical random graphs and the multiplicative coalescent. *Ann. Probab.*, **25**, 812–854.

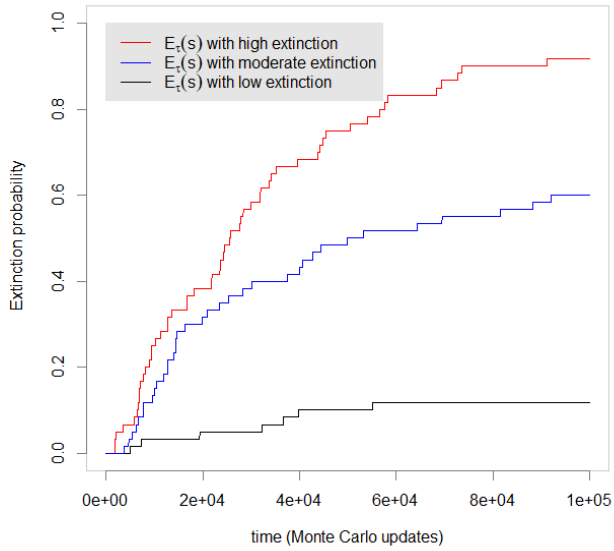

(a) $E_\tau(s)$ evolution during 10^5 updates

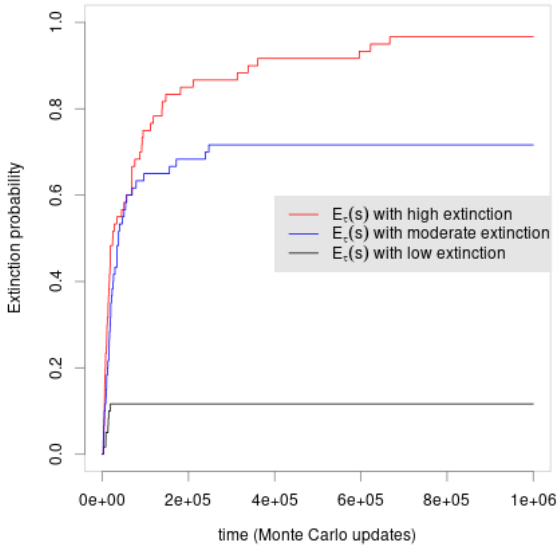

(b) $E_\tau(s)$ evolution during 10^6 updates

Figure 9: Time evolution of the extinction (discrete part $E_\tau(s)$) during 10^5 updates (left) and 10^6 updates (right) for the three extinction levels. The first (left) plot is within the transient phase. In the right plot the extinction probability has already reached a high level after 7×10^5 updates, but keeps on growing. We note that within the last period, the probability mass loss is much slower than the first period of the process.

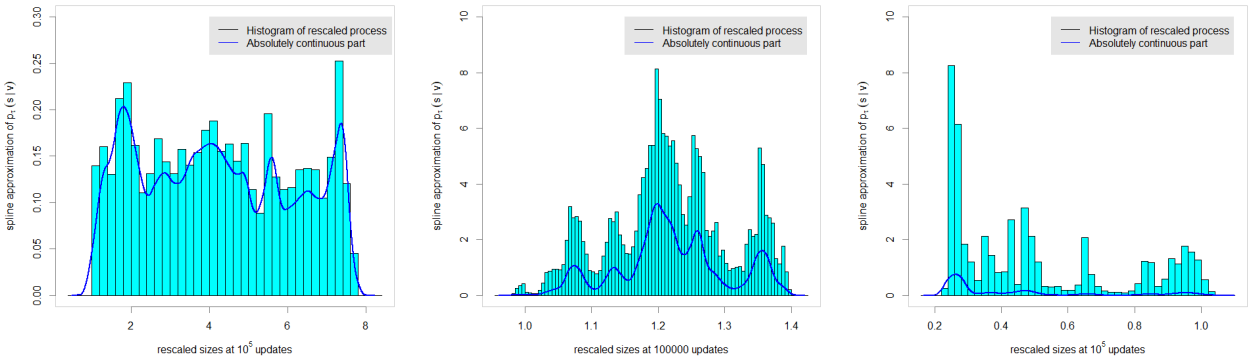

(a) $p_T(v|s)$ in low extinction $E_T(s) = 0.1166667$ (b) $p_T(v|s)$ in moderate extinction $E_T(s) = 0.6$ (c) $p_T(v|s)$ in high extinction $E_T(s) = 0.9166667$

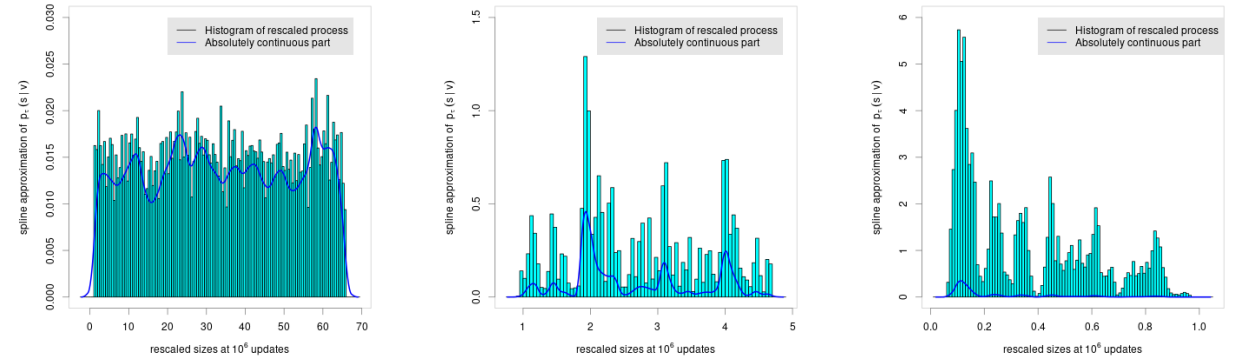

(d) $p_T(v|s)$ in small extinction $E_T(s) = 0.1166667$ (e) $p_T(v|s)$ in medium extinction $E_T(s) = 0.7166667$ (f) $p_T(v|s)$ in high extinction $E_T(s) = 0.9666667$

Figure 10: Spline approximations of the continuous part $p_T(v|s)$ during 10^5 updates (top) and 10^6 updates (bottom) for small, medium and large extinction levels for the network model. Particularly, we note in the right plots (high extinction case) that the high values of the continuous part near the absorbing point 0 induces a heavy flow of probability mass through this point, increasing the extinction probability.

Table 1: Maximum likelihood estimate $\hat{\theta}_\tau$ of M-spline coefficients θ_τ for the three data sets generated according to the Monte Carlo scheme with 10^5 updates.

Extinction	$E_T(s)$	Time: $\tau = T$ (updates)	Estimate $\hat{\theta}_\tau$ computed thanks to (4.10) (Summary of the rescaled process)			
			$(\min(V_n^\tau) = 0.9998333,\ \max(V_n^\tau) = 7.6955$ and $n = 100000)$			
Low	0.1166667	10^5	$\hat{\theta}_1^\tau = 2.174085 \times 10^{-10}$	$\hat{\theta}_2^\tau = 8.565083 \times 10^{-9}$	$\hat{\theta}_3^\tau = 1.543089 \times 10^{-4}$	$\hat{\theta}_4^\tau = 1.235168 \times 10^{-2}$
			$\hat{\theta}_5^\tau = 3.083254 \times 10^{-2}$	$\hat{\theta}_6^\tau = 3.282689 \times 10^{-2}$	$\hat{\theta}_7^\tau = 4.739526 \times 10^{-2}$	$\hat{\theta}_8^\tau = 4.484551 \times 10^{-2}$
			$\hat{\theta}_9^\tau = 3.227552 \times 10^{-2}$	$\hat{\theta}_{10}^\tau = 2.287612 \times 10^{-2}$	$\hat{\theta}_{11}^\tau = 2.788059 \times 10^{-2}$	$\hat{\theta}_{12}^\tau = 3.084818 \times 10^{-2}$
			$\hat{\theta}_{13}^\tau = 2.708257 \times 10^{-2}$	$\hat{\theta}_{14}^\tau = 2.775744 \times 10^{-2}$	$\hat{\theta}_{15}^\tau = 3.424341 \times 10^{-2}$	$\hat{\theta}_{16}^\tau = 3.583156 \times 10^{-2}$
			$\hat{\theta}_{17}^\tau = 3.750553 \times 10^{-2}$	$\hat{\theta}_{18}^\tau = 3.644205 \times 10^{-2}$	$\hat{\theta}_{19}^\tau = 3.240569 \times 10^{-2}$	$\hat{\theta}_{20}^\tau = 2.903384 \times 10^{-2}$
			$\hat{\theta}_{21}^\tau = 3.097417 \times 10^{-2}$	$\hat{\theta}_{22}^\tau = 1.860443 \times 10^{-2}$	$\hat{\theta}_{23}^\tau = 2.358073 \times 10^{-2}$	$\hat{\theta}_{24}^\tau = 3.767695 \times 10^{-2}$
			$\hat{\theta}_{25}^\tau = 2.062233 \times 10^{-2}$	$\hat{\theta}_{26}^\tau = 2.145072 \times 10^{-2}$	$\hat{\theta}_{27}^\tau = 2.371933 \times 10^{-2}$	$\hat{\theta}_{28}^\tau = 2.622918 \times 10^{-2}$
			$\hat{\theta}_{29}^\tau = 2.353721 \times 10^{-2}$	$\hat{\theta}_{30}^\tau = 2.381902 \times 10^{-2}$	$\hat{\theta}_{31}^\tau = 3.532589 \times 10^{-2}$	$\hat{\theta}_{32}^\tau = 4.651074 \times 10^{-2}$
			$\hat{\theta}_{33}^\tau = 8.670356 \times 10^{-3}$	$\hat{\theta}_{34}^\tau = 5.660394 \times 10^{-5}$	$\hat{\theta}_{35}^\tau = 3.203012 \times 10^{-8}$	$\hat{\theta}_{36}^\tau = 9.385657 \times 10^{-9}$
			$(\min(V_n^\tau) = 0.98,\ \max(V_n^\tau) = 1.399833$ and $n = 100000)$			
Moderate	0.6	10^5	$\hat{\theta}_1^\tau = 4.922400 \times 10^{-14}$	$\hat{\theta}_2^\tau = 2.849084 \times 10^{-9}$	$\hat{\theta}_3^\tau = 7.175060 \times 10^{-6}$	$\hat{\theta}_4^\tau = 4.0153420 \times 10^{-4}$
			$\hat{\theta}_5^\tau = 1.125218 \times 10^{-4}$	$\hat{\theta}_6^\tau = 2.875145 \times 10^{-5}$	$\hat{\theta}_7^\tau = 1.311450 \times 10^{-3}$	$\hat{\theta}_8^\tau = 2.643139 \times 10^{-3}$
			$\hat{\theta}_9^\tau = 3.742032 \times 10^{-3}$	$\hat{\theta}_{10}^\tau = 1.396266 \times 10^{-2}$	$\hat{\theta}_{11}^\tau = 1.306715 \times 10^{-2}$	$\hat{\theta}_{12}^\tau = 4.472780 \times 10^{-3}$
			$\hat{\theta}_{13}^\tau = 1.941370 \times 10^{-3}$	$\hat{\theta}_{14}^\tau = 6.508060 \times 10^{-3}$	$\hat{\theta}_{15}^\tau = 1.434618 \times 10^{-2}$	$\hat{\theta}_{16}^\tau = 9.115738 \times 10^{-3}$
			$\hat{\theta}_{17}^\tau = 5.459323 \times 10^{-3}$	$\hat{\theta}_{18}^\tau = 1.560724 \times 10^{-2}$	$\hat{\theta}_{19}^\tau = 2.770310 \times 10^{-2}$	$\hat{\theta}_{20}^\tau = 4.468627 \times 10^{-2}$
			$\hat{\theta}_{21}^\tau = 3.731368 \times 10^{-2}$	$\hat{\theta}_{22}^\tau = 3.229601 \times 10^{-2}$	$\hat{\theta}_{23}^\tau = 1.719026 \times 10^{-2}$	$\hat{\theta}_{24}^\tau = 2.047739 \times 10^{-2}$
			$\hat{\theta}_{25}^\tau = 3.375852 \times 10^{-2}$	$\hat{\theta}_{26}^\tau = 1.288016 \times 10^{-2}$	$\hat{\theta}_{27}^\tau = 9.920117 \times 10^{-3}$	$\hat{\theta}_{28}^\tau = 5.011079 \times 10^{-3}$
			$\hat{\theta}_{29}^\tau = 2.634596 \times 10^{-3}$	$\hat{\theta}_{30}^\tau = 3.763269 \times 10^{-3}$	$\hat{\theta}_{31}^\tau = 7.746913 \times 10^{-3}$	$\hat{\theta}_{32}^\tau = 2.066092 \times 10^{-2}$
			$\hat{\theta}_{33}^\tau = 2.032063 \times 10^{-2}$	$\hat{\theta}_{34}^\tau = 6.915656 \times 10^{-3}$	$\hat{\theta}_{35}^\tau = 3.937873 \times 10^{-3}$	$\hat{\theta}_{36}^\tau = 6.833797 \times 10^{-5}$
			$\hat{\theta}_{37}^\tau = 6.294704 \times 10^{-8}$	$\hat{\theta}_{38}^\tau = 4.162673 \times 10^{-9}$		
			$(\min(V_n^\tau) = 0.2341667,\ \max(V_n^\tau) = 1.029333$ and $n = 100000)$			
High	0.9166667	10^5	$\hat{\theta}_1^\tau = 5.707158 \times 10^{-9}$	$\hat{\theta}_2^\tau = 1.519021 \times 10^{-8}$	$\hat{\theta}_3^\tau = 1.131019 \times 10^{-4}$	$\hat{\theta}_4^\tau = 2.369929 \times 10^{-2}$
			$\hat{\theta}_5^\tau = 2.434907 \times 10^{-2}$	$\hat{\theta}_6^\tau = 1.687326 \times 10^{-3}$	$\hat{\theta}_7^\tau = 2.355056 \times 10^{-3}$	$\hat{\theta}_8^\tau = 2.710018 \times 10^{-3}$
			$\hat{\theta}_9^\tau = 2.080085 \times 10^{-3}$	$\hat{\theta}_{10}^\tau = 3.265613 \times 10^{-3}$	$\hat{\theta}_{11}^\tau = 6.049836 \times 10^{-3}$	$\hat{\theta}_{12}^\tau = 3.179036 \times 10^{-3}$
			$\hat{\theta}_{13}^\tau = 2.357804 \times 10^{-4}$	$\hat{\theta}_{14}^\tau = 1.402780 \times 10^{-4}$	$\hat{\theta}_{15}^\tau = 4.676280 \times 10^{-5}$	$\hat{\theta}_{16}^\tau = 9.136491 \times 10^{-4}$
			$\hat{\theta}_{17}^\tau = 1.801794 \times 10^{-3}$	$\hat{\theta}_{18}^\tau = 1.373335 \times 10^{-4}$	$\hat{\theta}_{19}^\tau = 2.815007 \times 10^{-5}$	$\hat{\theta}_{20}^\tau = 1.674692 \times 10^{-5}$
			$\hat{\theta}_{21}^\tau = 8.295516 \times 10^{-5}$	$\hat{\theta}_{22}^\tau = 1.081382 \times 10^{-3}$	$\hat{\theta}_{23}^\tau = 1.064029 \times 10^{-3}$	$\hat{\theta}_{24}^\tau = 6.632055 \times 10^{-4}$
			$\hat{\theta}_{25}^\tau = 2.208127 \times 10^{-3}$	$\hat{\theta}_{26}^\tau = 3.198497 \times 10^{-3}$	$\hat{\theta}_{27}^\tau = 1.944023 \times 10^{-3}$	$\hat{\theta}_{28}^\tau = 2.897280 \times 10^{-4}$
			$\hat{\theta}_{29}^\tau = 2.560822 \times 10^{-6}$	$\hat{\theta}_{30}^\tau = 1.362724 \times 10^{-10}$	$\hat{\theta}_{31}^\tau = 4.309607 \times 10^{-11}$	

Table 2: Maximum likelihood estimate $\hat{\theta}_\tau$ of M-spline coefficients θ_τ for the three data sets generated according to the Monte Carlo scheme with 10^6 updates.

Extinction	$E_T(s)$	Time: $\tau = T$ (updates)	Estimate $\hat{\theta}_\tau$ computed thanks to (4.10) (Summary of the rescaled process)			
			$(\min(V_n^\tau) = 0.9981667,\ \max(V_n^\tau) = 65.84017$ and $n = 1000000)$			
Low	0.1166667	10^6	$\hat{\theta}_1^\tau = 3.518104 \times 10^{-10}$	$\hat{\theta}_2^\tau = 1.112296 \times 10^{-7}$	$\hat{\theta}_3^\tau = 1.542933 \times 10^{-3}$	$\hat{\theta}_4^\tau = 2.185024 \times 10^{-2}$
			$\hat{\theta}_5^\tau = 2.275028 \times 10^{-2}$	$\hat{\theta}_6^\tau = 2.128447 \times 10^{-2}$	$\hat{\theta}_7^\tau = 1.992416 \times 10^{-2}$	$\hat{\theta}_8^\tau = 2.216032 \times 10^{-2}$
			$\hat{\theta}_9^\tau = 2.473679 \times 10^{-2}$	$\hat{\theta}_{10}^\tau = 2.685424 \times 10^{-2}$	$\hat{\theta}_{11}^\tau = 1.973229 \times 10^{-2}$	$\hat{\theta}_{12}^\tau = 1.666651 \times 10^{-2}$
			$\hat{\theta}_{13}^\tau = 1.838155 \times 10^{-2}$	$\hat{\theta}_{14}^\tau = 2.246801 \times 10^{-2}$	$\hat{\theta}_{15}^\tau = 2.483913 \times 10^{-2}$	$\hat{\theta}_{16}^\tau = 2.966979 \times 10^{-2}$
			$\hat{\theta}_{17}^\tau = 2.929490 \times 10^{-2}$	$\hat{\theta}_{18}^\tau = 2.277037 \times 10^{-2}$	$\hat{\theta}_{19}^\tau = 2.609092 \times 10^{-2}$	$\hat{\theta}_{20}^\tau = 2.787385 \times 10^{-2}$
			$\hat{\theta}_{21}^\tau = 2.387240 \times 10^{-2}$	$\hat{\theta}_{22}^\tau = 2.239408 \times 10^{-2}$	$\hat{\theta}_{23}^\tau = 2.012067 \times 10^{-2}$	$\hat{\theta}_{24}^\tau = 2.296877 \times 10^{-2}$
			$\hat{\theta}_{25}^\tau = 2.407899 \times 10^{-2}$	$\hat{\theta}_{26}^\tau = 2.200312 \times 10^{-2}$	$\hat{\theta}_{27}^\tau = 2.389224 \times 10^{-2}$	$\hat{\theta}_{28}^\tau = 2.441591 \times 10^{-2}$
			$\hat{\theta}_{29}^\tau = 2.088154 \times 10^{-2}$	$\hat{\theta}_{30}^\tau = 1.948037 \times 10^{-2}$	$\hat{\theta}_{31}^\tau = 2.250216 \times 10^{-2}$	$\hat{\theta}_{32}^\tau = 2.338947 \times 10^{-2}$
			$\hat{\theta}_{33}^\tau = 1.951102 \times 10^{-2}$	$\hat{\theta}_{34}^\tau = 1.924499 \times 10^{-2}$	$\hat{\theta}_{35}^\tau = 2.129246 \times 10^{-2}$	$\hat{\theta}_{36}^\tau = 2.331658 \times 10^{-2}$
			$\hat{\theta}_{37}^\tau = 3.276030 \times 10^{-2}$	$\hat{\theta}_{38}^\tau = 2.657141 \times 10^{-2}$	$\hat{\theta}_{39}^\tau = 2.740650 \times 10^{-2}$	$\hat{\theta}_{40}^\tau = 2.632676 \times 10^{-2}$
			$\hat{\theta}_{41}^\tau = 1.695569 \times 10^{-2}$	$\hat{\theta}_{42}^\tau = 1.075273 \times 10^{-3}$	$\hat{\theta}_{43}^\tau = 7.241221 \times 10^{-8}$	$\hat{\theta}_{44}^\tau = 2.872643 \times 10^{-10}$
			$(\min(V_n^\tau) = 0.9376667,\ \max(V_n^\tau) = 4.692667$ and $n = 1000000)$			
Moderate	0.7166667	10^6	$\hat{\theta}_1^\tau = 7.945395 \times 10^{-10}$	$\hat{\theta}_2^\tau = 3.232795 \times 10^{-9}$	$\hat{\theta}_3^\tau = 3.372351 \times 10^{-5}$	$\hat{\theta}_4^\tau = 8.431666 \times 10^{-4}$
			$\hat{\theta}_5^\tau = 5.501464 \times 10^{-3}$	$\hat{\theta}_6^\tau = 7.326125 \times 10^{-3}$	$\hat{\theta}_7^\tau = 6.924348 \times 10^{-4}$	$\hat{\theta}_8^\tau = 1.959284 \times 10^{-3}$
			$\hat{\theta}_9^\tau = 8.371880 \times 10^{-3}$	$\hat{\theta}_{10}^\tau = 2.643959 \times 10^{-3}$	$\hat{\theta}_{11}^\tau = 2.307764 \times 10^{-3}$	$\hat{\theta}_{12}^\tau = 2.569450 \times 10^{-4}$
			$\hat{\theta}_{13}^\tau = 9.043526 \times 10^{-4}$	$\hat{\theta}_{14}^\tau = 4.662708 \times 10^{-2}$	$\hat{\theta}_{15}^\tau = 3.412853 \times 10^{-2}$	$\hat{\theta}_{16}^\tau = 1.482417 \times 10^{-2}$
			$\hat{\theta}_{17}^\tau = 1.136030 \times 10^{-2}$	$\hat{\theta}_{18}^\tau = 9.867720 \times 10^{-3}$	$\hat{\theta}_{19}^\tau = 1.066432 \times 10^{-2}$	$\hat{\theta}_{20}^\tau = 1.477488 \times 10^{-3}$
			$\hat{\theta}_{21}^\tau = 8.770843 \times 10^{-4}$	$\hat{\theta}_{22}^\tau = 3.061089 \times 10^{-3}$	$\hat{\theta}_{23}^\tau = 5.289628 \times 10^{-3}$	$\hat{\theta}_{24}^\tau = 4.869629 \times 10^{-3}$
			$\hat{\theta}_{25}^\tau = 3.791995 \times 10^{-3}$	$\hat{\theta}_{26}^\tau = 3.054407 \times 10^{-3}$	$\hat{\theta}_{27}^\tau = 2.040948 \times 10^{-2}$	$\hat{\theta}_{28}^\tau = 7.911098 \times 10^{-3}$
			$\hat{\theta}_{29}^\tau = 2.205378 \times 10^{-3}$	$\hat{\theta}_{30}^\tau = 1.656508 \times 10^{-3}$	$\hat{\theta}_{31}^\tau = 3.088973 \times 10^{-3}$	$\hat{\theta}_{32}^\tau = 1.171999 \times 10^{-3}$
			$\hat{\theta}_{33}^\tau = 1.958612 \times 10^{-3}$	$\hat{\theta}_{34}^\tau = 2.489652 \times 10^{-3}$	$\hat{\theta}_{35}^\tau = 2.083094 \times 10^{-3}$	$\hat{\theta}_{36}^\tau = 4.914467 \times 10^{-3}$
			$\hat{\theta}_{37}^\tau = 2.636359 \times 10^{-2}$	$\hat{\theta}_{38}^\tau = 1.365230 \times 10^{-2}$	$\hat{\theta}_{39}^\tau = 6.812665 \times 10^{-3}$	$\hat{\theta}_{40}^\tau = 9.868614 \times 10^{-4}$
			$\hat{\theta}_{41}^\tau = 7.461842 \times 10^{-4}$	$\hat{\theta}_{42}^\tau = 3.190064 \times 10^{-3}$	$\hat{\theta}_{43}^\tau = 1.120269 \times 10^{-3}$	$\hat{\theta}_{44}^\tau = 1.623366 \times 10^{-3}$
			$\hat{\theta}_{45}^\tau = 2.186164 \times 10^{-4}$	$\hat{\theta}_{46}^\tau = 2.800214 \times 10^{-8}$	$\hat{\theta}_{47}^\tau = 1.811918 \times 10^{-9}$	
			$(\min(V_n^\tau) = 0.0615,\ \max(V_n^\tau) = 1.0$ and $n = 1000000)$			
High	0.9666667	10^6	$\hat{\theta}_1^\tau = 7.050851 \times 10^{-11}$	$\hat{\theta}_2^\tau = 9.422341 \times 10^{-9}$	$\hat{\theta}_3^\tau = 1.303347 \times 10^{-5}$	$\hat{\theta}_4^\tau = 2.262978 \times 10^{-3}$
			$\hat{\theta}_5^\tau = 9.718180 \times 10^{-3}$	$\hat{\theta}_6^\tau = 6.828396 \times 10^{-3}$	$\hat{\theta}_7^\tau = 2.687288 \times 10^{-3}$	$\hat{\theta}_8^\tau = 2.157739 \times 10^{-4}$
			$\hat{\theta}_9^\tau = 2.982128 \times 10^{-4}$	$\hat{\theta}_{10}^\tau = 1.454721 \times 10^{-3}$	$\hat{\theta}_{11}^\tau = 1.073393 \times 10^{-3}$	$\hat{\theta}_{12}^\tau = 1.298159 \times 10^{-4}$
			$\hat{\theta}_{13}^\tau = 2.236029 \times 10^{-4}$	$\hat{\theta}_{14}^\tau = 1.153824 \times 10^{-3}$	$\hat{\theta}_{15}^\tau = 8.586745 \times 10^{-4}$	$\hat{\theta}_{16}^\tau = 5.150211 \times 10^{-5}$
			$\hat{\theta}_{17}^\tau = 3.761612 \times 10^{-7}$	$\hat{\theta}_{18}^\tau = 6.207028 \times 10^{-4}$	$\hat{\theta}_{19}^\tau = 1.234211 \times 10^{-3}$	$\hat{\theta}_{20}^\tau = 2.891756 \times 10^{-4}$
			$\hat{\theta}_{21}^\tau = 2.922409 \times 10^{-4}$	$\hat{\theta}_{22}^\tau = 3.094402 \times 10^{-4}$	$\hat{\theta}_{23}^\tau = 3.413757 \times 10^{-4}$	$\hat{\theta}_{24}^\tau = 2.544367 \times 10^{-4}$
			$\hat{\theta}_{25}^\tau = 8.369699 \times 10^{-4}$	$\hat{\theta}_{26}^\tau = 4.639923 \times 10^{-4}$	$\hat{\theta}_{27}^\tau = 9.657284 \times 10^{-5}$	$\hat{\theta}_{28}^\tau = 7.847927 \times 10^{-5}$
			$\hat{\theta}_{29}^\tau = 5.129204 \times 10^{-6}$	$\hat{\theta}_{30}^\tau = 8.388677 \times 10^{-5}$	$\hat{\theta}_{31}^\tau = 1.383068 \times 10^{-4}$	$\hat{\theta}_{32}^\tau = 1.355711 \times 10^{-4}$
			$\hat{\theta}_{33}^\tau = 1.762992 \times 10^{-4}$	$\hat{\theta}_{34}^\tau = 5.217563 \times 10^{-4}$	$\hat{\theta}_{35}^\tau = 4.377643 \times 10^{-4}$	$\hat{\theta}_{36}^\tau = 4.195602 \times 10^{-5}$
			$\hat{\theta}_{37}^\tau = 2.134336 \times 10^{-6}$	$\hat{\theta}_{38}^\tau = 2.000416 \times 10^{-6}$	$\hat{\theta}_{39}^\tau = 2.119797 \times 10^{-6}$	$\hat{\theta}_{40}^\tau = 3.331573 \times 10^{-8}$
			$\hat{\theta}_{41}^\tau = 4.762100 \times 10^{-10}$	$\hat{\theta}_{42}^\tau = 6.445016 \times 10^{-12}$	$\hat{\theta}_{43}^\tau = 1.488554 \times 10^{-12}$	

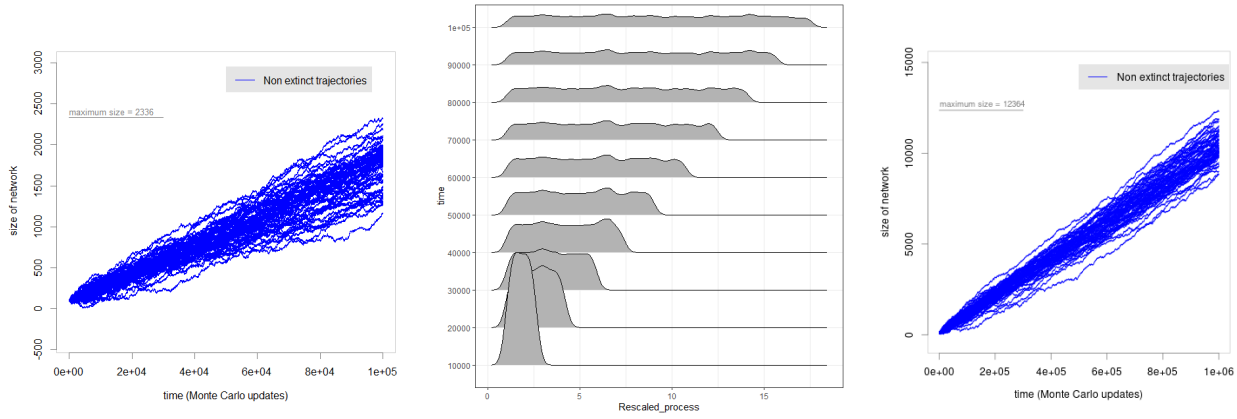

(a) Sample trajectories without extinction within 10^5 updates

(b) $p_\tau(v|s)$ evolution at 10 instants

(c) Sample trajectories without extinction within 10^6 updates

Figure 11: Time evolution of the number of nodes within 10^5 updates (left) and 10^6 (right) without observing any extinction. The plot in the center shows the time evolution of the density at 10 instants during 10^5 updates.

Atar R., Kang W., Kaspi H. & Ramanan K. (2021). Large-time limit of nonlinearly coupled measure-valued equations that model many-server queues with reneging. *Preprint, https://arxiv.org/abs/2107.05226.*

Bollobás B., Janson S. & Riordan O. (2007). The phase transition in inhomogeneous random graphs. *Rand. Struct. Algs*, **31**, 3–122.

Borgs C., Chayes J.T., Cohn H. & Holden N. (2018). Sparse exchangeable graphs and their limits via graphon processes. *Journal of Machine Learning Research*, **18**, 1–71.

Caron F. & Fox E.B. (2017). Sparse graphs using exchangeable random measures. *Journal of the Royal Statistical Society: Series B*, **79**, 1295–1366.

Chatterjee S. & Durrett R. (2009). Contact processes on random graphs with degree power law distribution have critical value zero. *Ann. Probab.*, **37**, 2332–2356.

Dawson D. (1993). Measure-valued Markov processes. Dans *École d'été de Probabilités de Saint-Flour XXI-1991. Lecture Notes in Mathematics, Vol. 1541*, réd. P.H. (eds), pp. 1–260. Springer-Verlag, Berlin, Heidelberg.

de Boor C. (2001). *A Practical Guide to Splines.* Applied Mathematical Sciences. Springer, Berlin.

Durante D., Dunson D.B. & Vogelstein J.T. (2017). Nonparametric Bayes modeling of populations of networks. *J. Amer. Statist. Assoc.*, **112**, 1516–1530.

Durrett R. (2007). *Random Graph Dynamics*. Cambridge Univ. Press, Cambridge.

Etheridge A. (2004). Survival and extinction in a locally regulated population. *The Annals of Applied Probability*, **14**, 188–214.

Goldenberg A., Zheng A.X., Fienberg S.E. & Airoldi E.M. (2010). A survey of statistical network models. *Foundations and Trends R in Machine Learning*, **2**, 129–233.

Hoff P.D. (2009). Multiplicative latent factor models for description and prediction of social networks. *Computational and Mathematical Organization Theory*, **15**, 261–272.

Hoff P.D., Raftery A.E. & Handcock M.S. (2002). Latent space approaches to social network analysis. *Journal of the American Statistical Association*, **97**, 1090–1098.

Hunter D.R., Goodreau S.M. & Handcock M.S. (2008). Goodness of fit of social network models. *J. Amer. Statist. Assoc.*, **103**, 248–258.

Kolaczyk E.D. (2009). *Statistical Analysis of Network Data: Methods and Models*. Springer, 1st edition.

Liggett T. (1985). *Interacting particle systems*. Springer, New York.

Luenberger D.G. & Ye Y. (2016). *Linear and Nonlinear Programming. Fourth Edition*. Springer International Publishing Switzerland.

Lusher D., Koskinen J. & Robins G. (2013). *Exponential Random Graph Models for Social Networks: Theory, Methods, and Applications*. Cambridge Univ. Press, Cambridge.

Mountford T., Mourrat J.C., Valesin D. & Yao Q. (2016). Exponential extinction time of the contact process on finite graphs. *Stochastic Process. Appl.*, **7**, 1974–2013.

Mountford T., Valesin D. & Yao Q. (2013). Metastable densities for contact processes on random graphs. *Electron. J. Probab.*, **103**, 1–36.

Norros I. & Reittu H. (2006). On a conditionally Poissonian graph process. *Adv. Appl. Probab.*, **38**, 59–75.

Penrose M. (2003). *Random geometric graphs*. University Press, Oxford.

Perry P.O. & Wolfe P.J. (2013). Point process modelling for directed interaction networks. *J. R. Stat. Soc. Ser. B. Stat. Methodol.*, **75**, 821–849.

Rastelli R., Friel N. & Raftery A.E. (2016). Properties of latent variable network models. *Netw. Sci.*, **4**, 407–432.

Schapira B. & Valesin D. (2017). Extinction time for the contact process on general graphs. *Probab. Theory Related Fields*, **3**, 871–899.

Schweinberger M. & Snijders T.A.B. (2003). Settings in social networks: A measurement model. *Sociol. Method.*, **33**, 307–341.

Sid-Ali A. & Khadraoui K. (2020). Weak convergence of a measure-valued process for social networks. *Preprint, arXiv:1809.04388*.

Stone C.J. (1990). Large-sample inference for log-spline models. *Annals of Statistics*, **18**, 717–741.

Ugander J., Karrer B., Backstrom L., & Marlow C. (2011). The anatomy of the facebook social graph. *Preprint, https://arxiv.org/abs/1111.4503*.

van der Hofstad R. (2017). *Random Graphs and Complex Networks*. Cambridge Univ. Press, Cambridge.

Veitch V. & Roy D.M. (2015). The class of random graphs arising from exchangeable random measures. *Preprint arXiv: 1512.03099*.

Wasserman S. & Faust K. (1994). *Social Network Analysis: Methods and Applications*. Cambridge Univ. Press, Cambridge.

Yuan B., Li H., Bertozzi A.L., Brantingham P.J. & Porter M.A. (2019). Multivariate spatiotemporal hawkes processes and network reconstruction. *SIAM Journal on Mathematics of Data Science*, **01**, 356–382.